STUDY OF SEMICONDUCTOR DETECTORS FOR SCANNING ELECTRON MICROSCOPE

by

Pappu Venkata Ramana

(September, 1966)

Submitted to the Department of Electrical Engineering in partial fulfilment of the requirements for the degree of Master of Science.

Department of Electrical Engineering
Faculty of Pure and Applied Science
University of Ottawa
Ottawa, Canada

1966.

CONTENTS

PAGE

LIST OF SYMBOLS

D_n, D_p	=	Diffusion constant for Electrons and holes respectively (cm^2/sec).
E	=	Strength of the Electrostatic field in the semiconductor (Volt/ cm).
E_G	=	Energy gap (ev)
I_B	=	Beam Current (amp)
J_n, J_p	=	Minority carrier current density composed of electrons or holes, respectively (amp cm^{-2}).
K	=	Boltzman's Constant = 1.38×10^{-22} joules per degree
ℓ	=	Distance from irradiated surface to the back surface of the Si wafer (cm).
L_n, L_p	=	Diffusion length for electrons and holes respectively (cm).
N_a, N_d	=	Density of ionized donors or acceptors respectively (cm^{-3}).
N_o	=	Number of electrons irradiating the surface of the semiconductor per second.
p_n, n_p	=	Minority carrier density in n and p layers respectively (cm^{-3}).
p_p, n_n	=	Majority carrier density in p and n layers respectively (cm^{-3}).
p , n	=	Minority carrier density in n and p layers respectively (cm^{-3}) after irradiation.
q	=	Electronic charge = 4.8×10^{-10} e. s. u.
r	=	Reflection coefficient.

s_n	=	Surface recombination velocity for electrons (cm/sec).
T	=	Absolute Temperature (degree K)
w	=	Distance from irradiated surface to the edge of the depletion layer within 'p' layer (cm).
x_j	=	Distance from irradiated surface to p-n junction (cm).
x	=	Distance from irradiated surface (cm).
V_B	=	Voltage of the incident electrons (Volt).
τ_n, τ_p	=	Minority carrier life time in p and n layer respectively (sec).
α	=	Absorption coefficient (cm^{-1}).
μ_n, μ_p	=	Conductivity mobility for electrons and holes respectively.

ACKNOWLEDGEMENTS

I wish to express my appreciation to Professor G. S. Glinski for making it possible to work on the microelectronics project at University of Ottawa. He suggested the project and supervised the work and I am thankful for his interest and help throughout this work.

Thanks are due to Dr. J.H. Simpson of the National Research Council for his inspiring discussions. Thanks are due to Prof. P. M. Thompson and Dr. W. Jirafe of the Department of Electrical Engineering for their comments, useful suggestions and considerable assistance in the experimental work.

I am thankful to Mr. B. Loro of the Northern Electric Company and to Dr. J.H. Simpson and Mr. Bolton of the National Research Council for fabricating the cells. Finally, I thank Mme LeBlanc for typing the manuscript.

This work was supported by the National Research Council of Canada through grant No. A-875 and the Defence Research Board under grant No. 5501-45.

ABSTRACT

This thesis is concerned with semiconductor radiation detectors for the detection of back-scattered and secondary electrons in a scanning electron microscopes.

The work consists of analysing, both theoretically and experimentally, Si p-n junction cells and Au-Si thin film contacts as regards their current gain when irradiated by electrons having energies in the range 4 to 8 Kev. The current gain, in both photovoltaic and photodiode modes is obtained and was of the order of 1000. This device virtually acts as a high gain amplifier with an electron beam as its input.

Introduction:

In a scanning electron microscope an electron beam of a small diameter is scanned over the surface of an object and the emitted electrons are detected. It is convenient to classify the electrons, emitted from the surface of the object as a result of the bombardment by the primary electron beam into two classes according to their velocities.

1) Secondary Electrons
2) Reflected Electrons

The secondary electrons have energies of only a few electron volts and for the purposes of measurement are usually taken as all electrons with energies less than 50 ev. The reflected electrons have energies between 50 ev. and the primary beam energy.

The fraction of the primary electron current that is reflected from the object depends on [1]

1) Atomic Number 'z'
2) Angle of incidence.

It is independent of primary beam energy. It increases as z increases and also as the angle of incidence.

The secondary electrons depend on the primary beam energy. It has been shown that clean metal targets exhibit a universal variation of secondary emission with the primary electron energy, if experimental values of secondary emission coefficient and primary energy are properly normalized.

In a typical system the total current leaving the object is of the order of 10^{-8} to 10^{-9} amps. Because of this, a sensitive detector must be employed for collecting them. Three methods of collection have been investigated.

1) Electron multipliers
2) Scintillation detectors
3) Semiconductor detectors

In chapter 1, a short description of electron scanning microscope is given and then, the collection of back scattered electrons is discussed using electron multipliers and scintillation counters. Then the collection of these electrons by semiconductor detectors is discussed. In chapter 2, among these semiconductor detectors three types are discussed:

1) Metal semiconductor rectifying junctions
2) Semiconductor p-n junctions
3) Metal oxide semiconductor cells

Then the three collection systems are compared. In chapter 3, the physical principles of Si p-n junctions are discussed in photovoltaic and photodiode modes. The effect of surface recombination velocity and the type of radiation etc. on the photo-current are discussed. Also the effect of radiation damage and temperature is discussed.

In chapter 4, the experimental arrangement and the discussion of the results are given.

A concluding discussion is presented in Chapter 5.

REVIEW OF COLLECTION SYSTEMS

1.1 Scanning Electron Microscope:

Various descriptions of scanning electron microscopes have been published during the last few years [2]. A schematic diagram of the scanning electron microscope is shown in Figure 1(a). The main body of the instrument is a vacuum chamber which houses the electron gun and the electrostatic lenses. These produce a focussed electron beam spot, on the specimen about .1 micron in diameter. Deflecting plates are located in the column so that the beam can be moved in a television type raster over the specimen. The deflecting plates are driven by a scanning generator. This same scanning signal is fed to a cathode ray tube. Thus the cathode ray tube is scanned in synchronism with the primary beam scanning the specimen.

With a 0.1 micron spot and 1000 line raster an area of 100 by 100 microns can be scanned. This can be increased up to millimeter square with an accompanying increase in beam spot size. As the primary electron beam scans the specimen, the reflected and secondary electrons are emitted from the specimen. Either secondary or reflected electrons can be collected and used to intensity modulate the cathode ray tube. Thus scanning electron microscope can be used for the surface inspection of e.g. micron sized thin film components. The experimental details of the collection systems are discussed in the next section.

As mentioned above the number of reflected electrons depends on the average atomic number as shown in Fig. (1)b, which is determined by chemical composition of the specimen and topography of the portion of the specimen under examination.

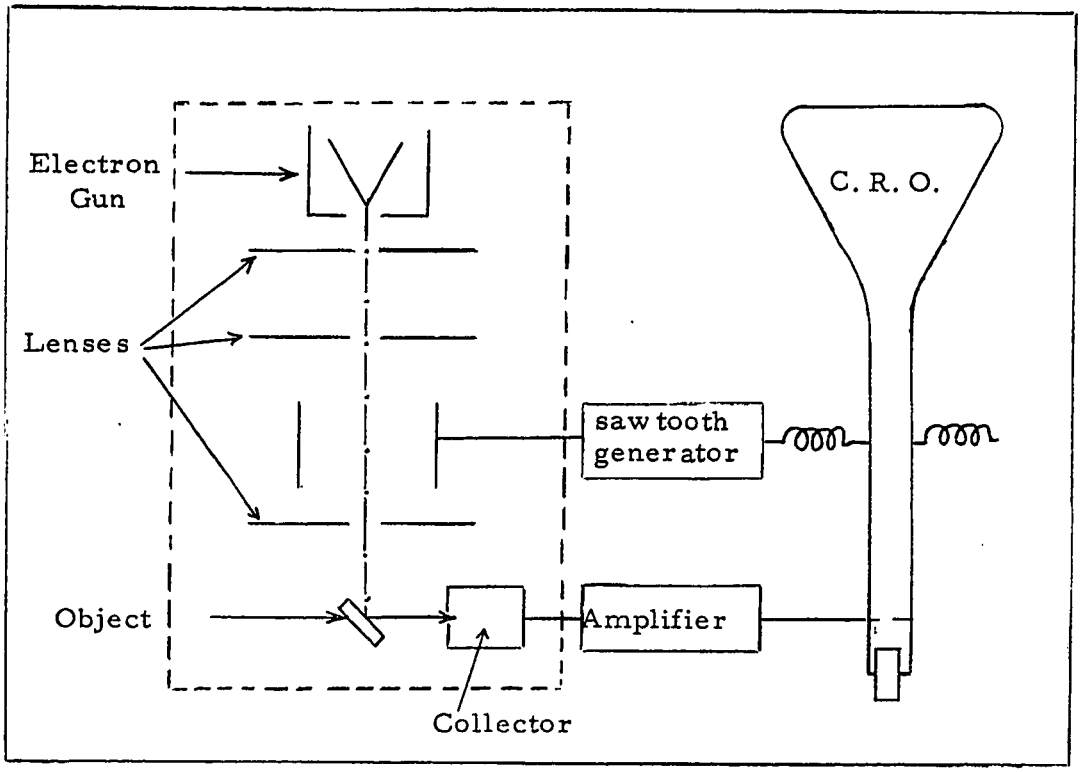

Figure 1(a) Schematic of Electron Scanning Microscope.

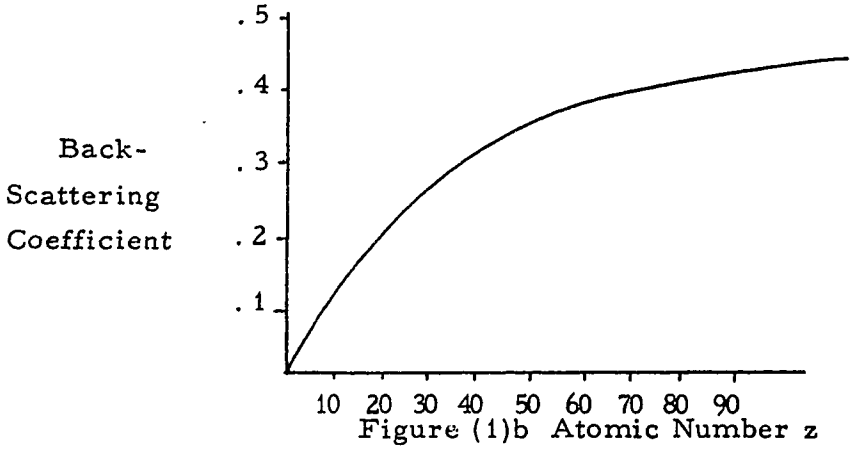

Figure (1)b Atomic Number z

The reflected electron image due to the above two effects can be separated by using two identical electron detectors. This is done by either adding or subtracting the outputs from a pair of matched collectors placed opposite each other.[15]

1.2 Electron Collection Systems:

As mentioned above, in a scanning electron microscope either reflected or secondary electrons can be used to intensity modulate the cathode ray tube. The collection of reflected and secondary electrons separately, are described as follows[3].

1.2.1 Electron Multipliers:

The electron multipliers are used as electron detectors. The electrons that are emitted from the specimen by the bombardment of the electron beam, fall on the first dynode of the electron multiplier and the output from this device is amplified and applied to the cathode ray tube for the image. Because of its size, the electron multiplier cannot be placed very near to object and the solid angle subtended at the object by the first dynode is not large. Thus only a small percentage of the

emitted electrons are collected and the efficiency of the collection is not high.

1.2.2 Scintillation Counters:

It has been advantageous to replace the electron multiplier as a detector by a combination of a scintillator and photomultiplier. In this case a small hemisphere of scintillating material is mounted quite close to the object and the light of the scintillator is conveyed to the multiplier by a light pipe. The light output from the scintillator is proportional to the energy of the electrons striking it. With the arrangement described above, both secondary and reflected electrons leaving the object over a wide solid angle strike the scintillator but the reflected electrons are much more effective in producing light than secondaries. Thus the output signal from the photomultiplier is generated almost entirely by reflected electrons.

The secondary electrons can be detected separately in the following manner. The detection is the same as for reflected electrons, but the secondary electrons are accelerated first and then collected. In a typical detection system the scintillator is enclosed in a metal box which the electrons enter through an aperture covered with metal gauze. The box is maintained at a small positive potential with respect to the object and is so placed that relatively few of the reflected electrons enter the aperture. Within the box, the scintillator is kept at a positive potential of 10 kev above that of the box and all the electrons passing through the aperture are accelerated towards the scintillator and are given sufficient energy to produce many photons. Since the photons which reach the photo cathode, via

light pipe, produce more electrons than initially struck the scintillator little additional noise is introduced by the scintillator photomultiplier combination. With the arrangement described above it is possible to produce a final image of the object, the contrast of which is controlled either by secondary or reflected electrons.

1.2.3 Semiconductor Detectors:

When high energy electrons are absorbed by a semiconductor, they dissipate most of their energy by ionizing the atoms of the solid. The high energy electrons lose their energy in a series of excitation processes in the semiconductor so that many electron hole pairs will be produced. These carriers can be collected if a rectifying junction or barrier is present. These carriers induce a voltage across the junction and this phenomenan is known as photovoltaic (electron voltaic) effect. If such a junction is reverse biased, then it is known as photodiode. Thus photovoltaic cells and photodiodes are effective detectors of electrons [4]. Three types of semiconductor detectors are discussed.

1) Metal semiconductor rectifying junction
2) P-n junctions
3) Metal oxide semiconductor cells.

The first two are similar in operation, but differ in the formation of the junction. The principles of the formation of these junctions mentioned above are discussed in the next chapter, and their relative advantages as collection systems are compared.

CHAPTER 2

SEMICONDUCTOR DETECTORS

As mentioned in the previous chapter, the carriers that are generated, when a semiconductor is subjected to irradiation, can be collected if a rectifying junction is present. A rectifying junction can be formed by the following two methods[5].

(1) p-n junction formed by the introduction of a suitable type impurity into the opposite type semiconductor.

(2) Metal semiconductor barrier formed by deposition of a suitable transparent metallic film by evaporation as in a selenium cell.

2.1 Semiconductor p-n Junction:

Germanium and silicon, both have four valence electrons in their crystalline form. If an impurity of the fifth group material from the periodic table e.g. arsenic is added, then the impurity atom replaces the silicon atom and is left with an extra unattached electron. The energy required to remove the electron from the impurity is quite small and thermal energy is sufficient for this purpose. Thus the electron moves freely in the crystal and contributes electrical conductivity just as in metals. The conductivity in a semiconductor with group five impurities is due to these excess electrons, that is, negative charges and the material is called 'n' type semiconductor.

If the impurity atom in the crystal is a group three element from the periodic table, e.g. boron, then the impurity atom replaces the silicon atom but does not have sufficient electrons

to complete all the valence bonds. An electron from a nearby atom will move over to complete the bond leaving behind another uncompleted bond. This empty position is called a hole. Materials with group three impurities have an increased conductivity due to these holes or positive charges, and are called p type semiconductors.

When a single crystal of semiconductor contains a higher concentration of n type than p type impurities while in the remainder, the p type impurities predominate, a p-n junction is formed. The electrons and holes diffuse from regions of high concentration as gas diffuses, i.e. electrons from the n side and holes from the p side, in the vicinity of the junction intermingle by diffusion, leaving behind a dipole layer due to fixed charges of the impurities. This built-in field is important for the operation of photovoltaic cells.

2.1.1 Irradiation Effects in p-n Junctions:

When a semiconductor is irradiated by high energy electrons, a photoconductive current can be produced in the body of the semiconductor, if an electric field is applied to it during the irradiation process. If the semiconductor contains a p-n junction its built-in field can be used instead of externally applied field to produce the photocurrent when the junction is irradiated. The method by which this is accomplished can be demonstrated by means of the electron energy diagram of Fig (2). The junction is subjected to irradiation in the region shown by the arrows and hole electron pairs are

produced on both sides of the central plane AA.

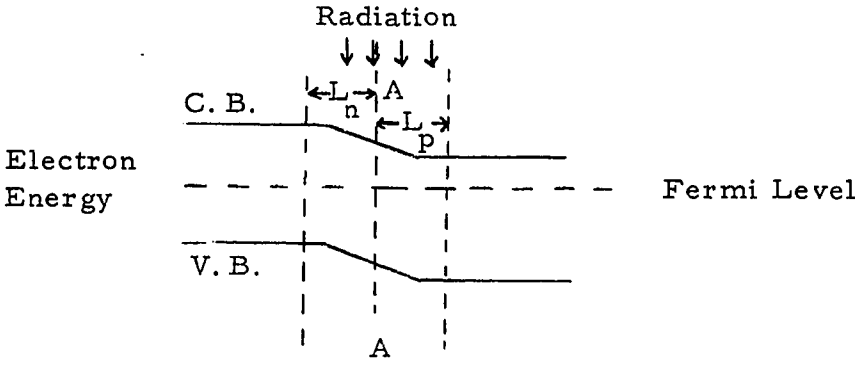

Fig. (2) Electron Energy diagram illustrating the operation of a photovoltaic cell.

Electrons generated within a diffusion length from AA, in the p region are swept by the built-in field into n region. Similarly holes undergo a similar process and move into p region. If it is connected to an external circuit a current is produced therein. If no connections are made to it, a potential will exist between its terminals, as long as the radiation persists, because of the separation of charge produced by the junction.

The reverse biased p-n junction is also used as a detector of radiation [4]. The minority carriers produced in the neighbourhood of the junction by the incident radiation are swept rapidly away to produce a current in the external circuit that is very much larger than the reverse current flowing in the absence of radiation. The junction is thus an efficient radiation detector.

2.2 Metal Semiconductor Barrier:

Rectification phenomena originating at the contact between a metal and a semiconductor has been observed for many years. These contacts have been used as rectifiers and photodetectors.[4] A brief theory of such contacts on Germanium and Silicon is given below.

The rectification theory postulates the existence of a space charge region in the semiconductor, adjacent to the metal, which forms a barrier to the electronic flow. This barrier is depicted for n type material as shown in Figure (3).

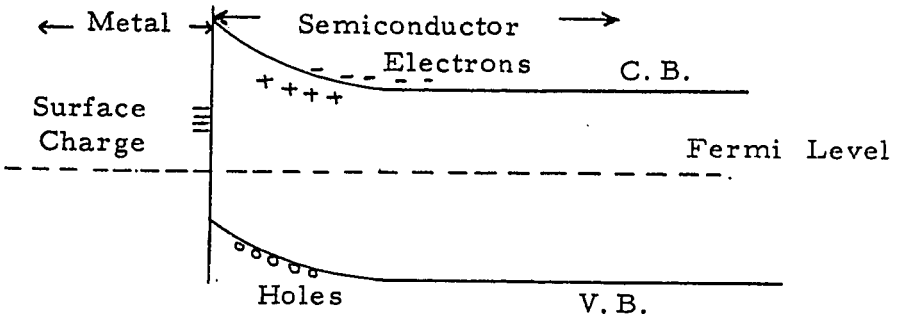

Fig. (3). Electron energy level diagram of a metal semiconductor contact.

The establishment of such a barrier will be expected to occur if the work function of the metal is higher than that of the semiconductor. This would imply that as the metal and semiconductor are originally brought into close proximity, it will be easier for an electron to escape from the semiconductor to the metal than vice versa, so that previously neutral semiconductor

will acquire a net positive charge and the metal will acquire a corresponding net negative charge. The dipole set up by these charges will create an electric field which will enhance the escape rate of the electrons from the metal and retard the escape rate of electrons from the semiconductor when the field has just become sufficient to make these two escape rates equal, no further net transfer charge will occur and the system will reach thermal equilibrium. Because of the relatively low concentration of the free carriers in the semiconductor, the space charge region extends to a considerable depth into the semiconductor approximately 10^{-6} to 10^{-4} cm where as the charge residing in the metal will constitute a surface charge. Thus a rectification contact can be obtained by the combination of a metal and semiconductor.

In the above description it is assumed that the work function of the metal is higher than that of the n type semiconductor. If the work function of the metal is lower than that of the semiconductor, the net transfer of electrons in the process of establishing equilibrium will be from the metal to semiconductor. This will result in an accumulation of electrons in the semiconductor region adjacent to the metal. The impedance of this region will be thus lower than n type bulk, resulting in a low resistance contact. If the current voltage characteristic is taken, the voltage will be mainly across the bulk of the semiconductor and result in an ohmic curve.

Similarly if the semiconductor is p type, and for rectification, the work function of the p material must be higher than that of the metal. If the p type semiconductor work function is lower than that of the metal, then an ohmic contact will be obtained.

Thus the nature of the rectification contact depends strongly on the work function of the metal used to make the contact. The following is the list of work functions and rectification properties of metals [4(d)].

Table 1

Metal	Work Function	N type Silicon	P type Silicon
Al	3.74	Ohmic	Rectifying
Pb	4.02	Ohmic	Rectifying
Au	4.57	Rectifying	Ohmic
Pt	5.29	Rectifying	Ohmic

Work Functions and Rectification properties of metals plate onto 2.5 ohm cm n and p silicon.

Irradiation Effects In Metal Semiconductor Barrier:

If a metal semiconductor barrier is subjected to irradiation, a photocurrent can be produced. The method by which this is accomplished can be demonstrated by means of the electron energy diagrams of Fig. (4). A metal semiconductor contact without bias and without irradiation is shown in Fig. (4)a . Under these conditions no current will flow across the barrier and the hole concentration 'p_n' in the

semiconductor will balance the hole concentration 'C_o' in the metal.

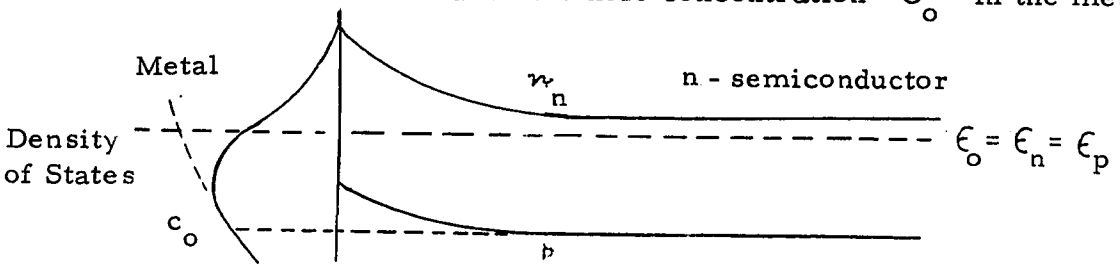

Fig 4(a) Dark Metal Semiconductor Contact.

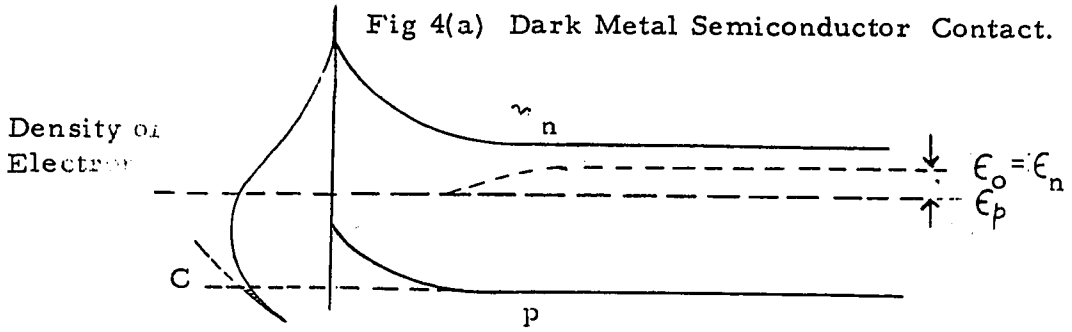

Fig 4(b) Irradiated - Open Circuited Contact.

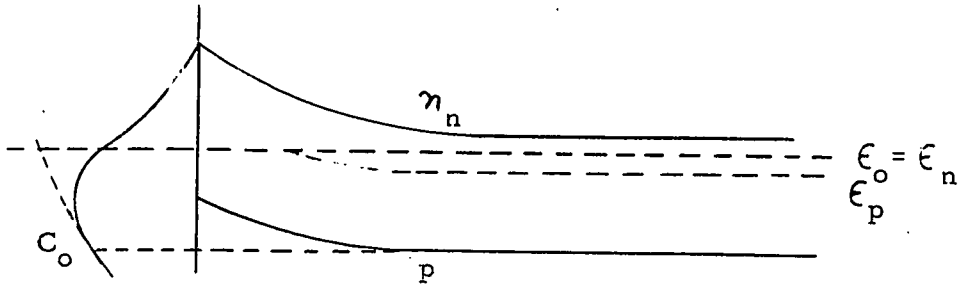

Fig 4(c) Irradiated - Short Circuited Contact.

It is assumed that the barrier is high enough to keep any electron interchange from taking place over the top of the barrier. ϵ_o is the Fermi level in the semiconductor which determines the relative magnitudes of n_n and p_p.

Fig. (4)b shows the same diode under electron irradiation with its terminals open. It is assumed that the density of minority carriers generated is small compared with the majority carrier density n_n. The hole density p is increased and thermodynamic equilibrium no longer exists across the energy gap. Since the diode is open no current will flow, so the semiconductor side of the diagram must be raised until the enhanced hole distribution p is balanced by an equal number of holes c in the metal. The difference between the position of the Fermi level in the metal and the old Fermi level in the semiconductor is the photovoltage v.

The hole distribution c is determined by the Fermi level in the metal. The new equilibrium condition is achieved by matching hole distributions under the barrier. This means that the hole distribution p in the semiconductor is compatible with a Fermi level at the same energy as the Fermi level in the metal. Such a hypothetical Fermi level is called a quasi Fermi level and is shown by the dashed line ϵ_p in Figure (4b). The electron distribution 'n_n' has not been increased by the irradiation so that it is compatible with the old Fermi level ϵ_o. If there is a ohmic contact to the semiconductor, thermodynamic equilibrium will be enforced at this contact and the Quasi Fermi level coincideswith the true Fermi level ϵ_o. The voltage measured between the metal and this ohmic contact will be the photoelectric voltage.

Figure (4c) shows the same diode when its terminals short circuited. A hole diffusion current density J_p flows into the metal. If a reverse bias is applied to this junction, then due to the increased potential gradient, the motion of the electron hole pairs in the field towards the junction and the collection of electron hole pairs are improved. The junction is thus an efficient radiation detector.

2.3 Metal-Oxide Semiconductor Cells:

These cells also can be used for the detection of electrons. A brief description of the theory of these cells is discussed below [6].

The electrode geometry and the circuit connections of the cell are shown in Fig. (5). The cell consists of a Si either p or n type covered with a SiO_2 layer about a micron thick, over this, a transparent metallic film .

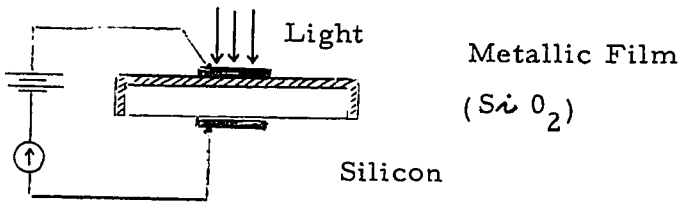

Figure (5).

Light enters through the metallic film, passes through the oxide and is absorbed by the silicon. For light of sufficient energy, the excited electrons so produced, are raised into the conduction band of the $Si\ o_2$. If a suitable bias voltage is applied

across the oxide, they move through the layer and are measured as current. Other kinds of radiation such as high energy electrons can also be used. The cell is biased to make the silicon negative and the metal electrode positive. When the specimen is irradiated by light, a steady current is observed.

Such kind of current can be produced by several mechanisms. These are :

1) Photoemission of electrons from the valence band of Si into the conduction band of $Si\,o_2$.
2) Photoconductivity processes in the $Si\,o_2$ due to light absorbed within the oxide itself.
3) Photoemission of holes from the metal electrode into the valence band of $Si\ o_2$.

It has been shown that the photocurrent is entirely due to first process i.e. emission of electrons from Si into $Si\,o_2$. Also it has been shown that the photocurrent is not due to any of the other two mechanisms. Since $Si\,o_2$ is a good insulator, the dark current will be low (of the order of 10^{-12} Amp (cm^2)). The photocurrent as a function of applied voltage is shown in Figure (6) for n and p type crystals. It is found that the curves are similar in nature. There is no detectable current at low voltages. This is followed by steeply rising curve and saturated at high voltages. From the spectral response of the photocurrent, a photoemission threshold of 4.25 ev is obtained, independent of whether the silicon is n or p type.

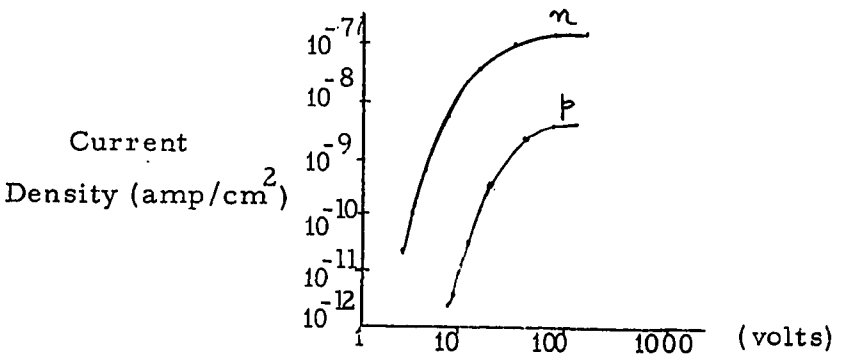

Fig. (6). Photo current vs. applied voltage

This cell would not be expected to have a high collection efficiency compared with diffused p-n junctions for several reasons.

1) The effective penetration of the high energy electrons is blocked by the layer of $Si\ 0_2$.

2) The ionization potential (i.e. raising an electron from the Si valence band to the conduction band) is larger than the Si p-n junction.

Si P-n junction	E = 3.7 ev[9]
Si-si o_2 cell	E = 4.25ev

But the advantage of these cells is that the dark current is smaller than the Si p-n junctions. Thus the metal oxide semiconductor cells can be used for the detection of electrons.

2.4 Comparison of the Collection Systems.

As mentioned in Chapter 1, the combination of scintillator and photomultiplier is superior to electron multipliers because of its size. The electron multiplier cannot be placed very near to the object and the solid angle subtended at the object by the first dynode is not large. Thus only a small percentage of emitted electrons are collected and thus the efficiency of the collection is not high.

In the case of scintillation counter, the electrical energy is first converted into light energy by a plastic scintillator. And the light energy is transmitted through a light pipe on to the photo-cathode of the photomultiplier. The conversion efficiency of the scintillator falls as the incident particle energy is reduced below 50 Kev. It was found that the response varied linearly with incident energy for energies above a threshold value which varied between 2 to 10 Kev as shown in figure (7) [7]. And also it has been shown that the method used to prepare the scintillator was of critical importance, in determining the performance of the scintillator for low incident energy electrons.

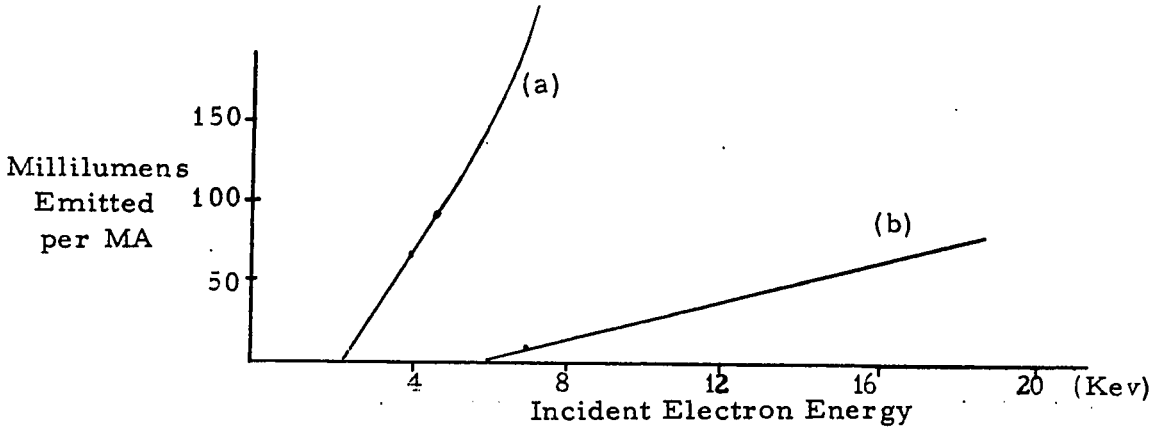

Figure (7) Scintillator Performance.

Current (a) wet machined curve (b) dry machined with metal polish.

Finally, the optical efficency of the scintillator light pipe system does not exceed 40% depending upon the length of the light pipe[7].

In some cases it is impracticable to couple the scintillator directly to the photomultiplier. In this a light guide is used to transmit the light from the scintillator to the photocathode. The properties and design of light guides are such that there should be minimum light losses. If the scintillator diameter is less than that of the light guide, a light coupler of appropriate shape should be inserted . It has been observed [7(a)], that the transmission efficency of 1" dia. and 10" long light guide is about 40% and also the efficiency depends upon the type of the coupler used. Minimum loss occurs when the scintillator is coupled directly to the photomultiplier.

In the case of Si p-n junction cells can be used, to collect these electrons directly, i. e. electrical energy is not converted into light energy and then light energy into electrical energy. there is no threshold value of the incident energy of collected electrons.

The frequency response of Si p-n junction cells is much higher than that of the frequency response of the scintillation counters which is set by the decay time of the scintillator or by the transit time spread of the photomultiplier. It is possible to obtain a frequency response up to 1 K M c/s for photocells, where the frequency response of the scintillation counter is of the order of 1 M c/s.

Finally the size of the semiconductor diode can be smaller than the size of the scintillation counters.

Summarizing the above discussion, semiconductor cells are superior with respect to scintillation counters in sensitivity, frequency response and the size and are able to detect low energy electrons.

CHAPTER 3

PHYSICS OF SEMICONDUCTOR CELLS

As mentioned in the previous Chapter, the photovoltaic cell and the reverse biased photovoltaic cell can be used for the detection of electrons. The analysis of these two cells is discussed in this Chapter.

3.1 Photovoltaic Cell:

When a semiconductor p-n junction is subjected to irradiation by an electron beam, the electrons interact with the atoms of the solid and they dissipate most of their energy. Carriers generated are in excess of the number permitted by thermodynamic equilibrium. These carriers induce a voltage across the junction. This phenomenon is called electron (photo) voltaic effect [5].

To illustrate the nature of the electron voltaic effect Figure (8a) shows the cross section of a p-n junction irradiated by electrons, while Figure (8b) shows the junction in equilibrium and during irradiation respectively. At equilibrium the Fermi level is continuous across the junction, so that the extra holes on p side and electrons on n side intermingle by diffusion and recombine leaving behind a dipole layer due to fixed charges of the impurities. This built-in potential is important in the operation of such devices as solar cells. The height of the potential difference is equal to the difference between the location of the Fermi level on n and p sides at a large distance from the junction.

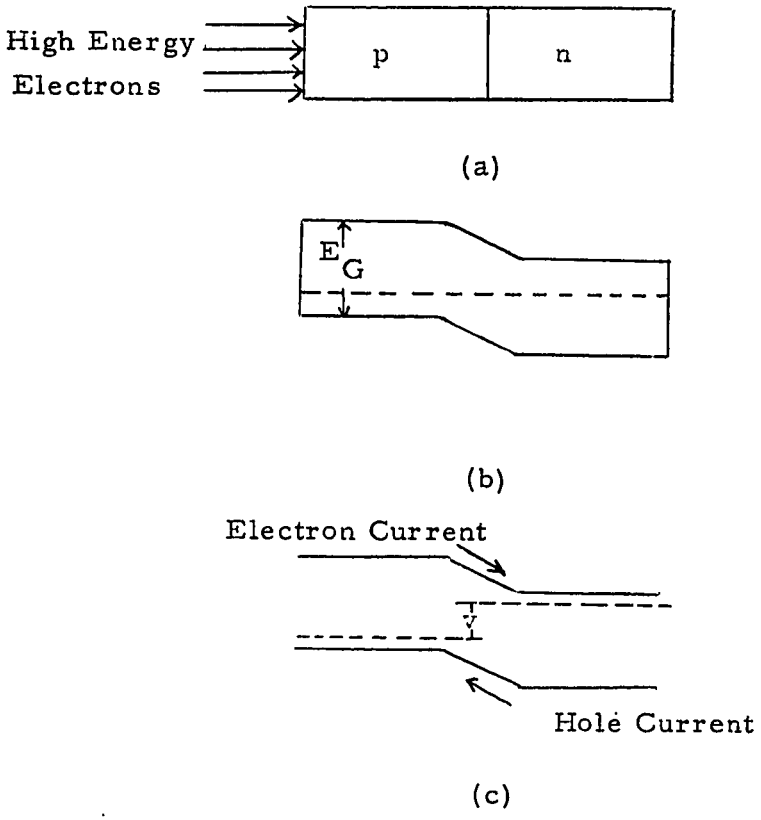

Figure (8)

If the junction is irradiated, electron hole pairs produced in the semiconductor are separated by the built-in field. The separated pairs bias the junction in the forward direction, as shown in Figure (8c), and deliver power to the load. Since each electron produces many pairs, the junction cell converts a small current of high energy electrons to a much larger current of low energy electrons.

If the load is infinite, the current is zero and the voltage has its maximum value, V_{max}. As the impedance is decreased,

there is a net flow of current into the load, until, when a short circuit is placed across the junction. The maximum current I_s will flow through it and $V = 0$.

In the following sections, the electron voltaic effect and the efficiency of the cell in terms of the parameters of the semiconductor are considered. The expression for the photocurrent in terms of these parameters is derived from the plane geometry of the cell. The effects of surface recombination velocity and bulk recombination, on the photocurrent are discussed. In general the diffusion length or sum of the diffusion lengths of electrons and holes must be large compared to the range over which the electrons are absorbed. For maximum efficiency a low dark current is desirable. A large energy gap is also desirable because it is an upper limit for the attainable cell voltage and also large energy gap results in a low dark current.

3.2 Analysis of the Electron Voltaic Effect:

The equations governing the electron voltaic effect can be deduced from the equivalent circuit of an irradiated rectifying junction as shown in Fig. (9)

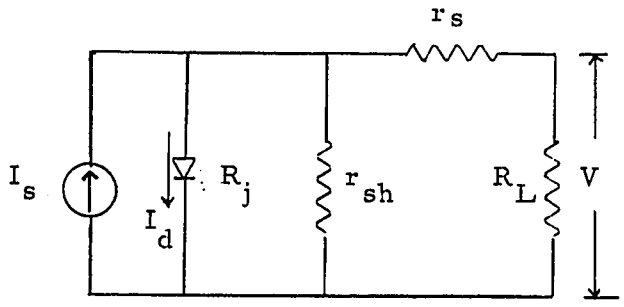

Figure (9)

The circuit consists of a constant current source, delivering a current I_s into a network of impedances which include the non-linear impedance of the junction R_j, the series resistance r_s, the shunt resistance r_{sh} and the load resistance R_L .

The parameters I_s and I_j are explained below:

a) The ionization radiation i.e the high energy electrons V_B with beam current I_B, after interacting with the solid generates a constant current I_s.

b) The junction has a current voltage characteristic of the form

$$I_j = I_o \left(e^{\frac{qv}{KT}} - 1 \right) \qquad (1)$$

where I_j is the current through the junction, I_o is the reverse saturation current of the diode, V is the voltage across it and its effective impedance R_j is given by

$$R_j = \frac{\partial v}{\partial I_j} = \frac{e^{-\lambda v}}{\lambda I_o} \quad \text{where } \lambda = \frac{q}{KT} \qquad (2)$$

The circuit analysis can be simplified by noting that when maximum power is transferred to the load resistance R_L, then $R_L < r_{sh}$ and $R_L > r_s$. The first condition is easy to attain since generally $r_{sh} >> 10^4$ ohms. The second condition can be realized in practice by using a geometry in the device which produces r_s values in the desired range. The simplified circuit is shown in Figure (9b)

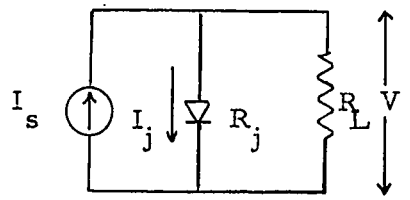

Figure (9b).

It is evident from the diagram that the current passing through R_L is the difference between I_s and I_j. A current voltage diagram which illustrates this relation is shown in Figure (10).

$$I = I_s - I_o\,(e^{\lambda v} - 1) \qquad (3)$$

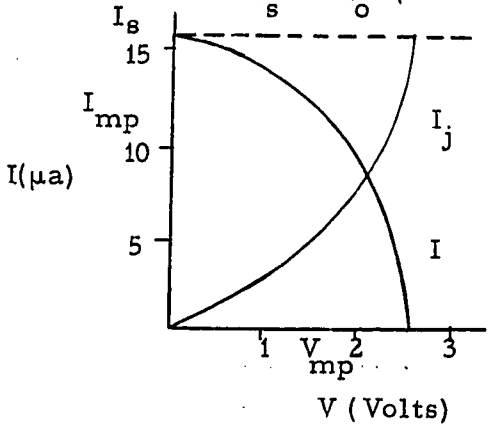

The constant current generator is represented by the line I_s, the junction i-v characteristic equation 1, by I_j curve and I, by the difference of these two. The three parameters which are measurable by experiment are also shown in the diagram. They are: open circuit voltage, V_{max}, the short circuit current I_s, and the dark current I_o which can be determined from the slope of the i-v characteristic at V=o

$$(i.e) \qquad \left.\frac{\partial i}{\partial v}\right|_{v=o} = -\lambda I_o \qquad (4)$$

From equation (3) it follows that

$$\left(\frac{I_s}{I_o} + 1\right) = e^{\lambda v_{max}}$$

$$i.e \qquad V_{max} = \frac{1}{\lambda} \ln\left(\frac{I_s}{I_o} + 1\right) \qquad (5)$$

In terms of these parameters, the voltage and current at maximum power can be determined by equating the load impedance to the

impedance of the junction as given by equation (2)

$$R_{mp} = \frac{v_{mp}}{i_{mp}} = \frac{e^{-\lambda v_{mp}}}{\lambda I_o} \qquad (6)$$

Equation (3) can be written as

$$I_s = I + I_o(e^{\lambda v} - 1)$$

By combining equations (3) & (6) and comparing to equation (5), we get

$$e^{\lambda v_{mp}} (1 + \lambda v_{mp}) = (\frac{I_s}{I_o} + 1) = e^{\lambda v_{max}} \qquad (7)$$

Appropriate substitutions yield the following expressions for the current at maximum power and the maximum power dissipated in the load, respectively

$$i_{mp} = \frac{\lambda v_{mp}}{(1 + \lambda v_{mp})} (1 + \frac{I_o}{I_s}) I_s \qquad (8)$$

$$P_{max} = I_o \lambda v_{mp}^2 e^{\lambda v_{mp}} \qquad (9)$$

The maximum efficiency, η_{max}, is the ratio of P_{max} to the input power, $P_i = \frac{v_B I_B}{q}$ so that

$$\eta_{max} = (1 + \frac{I_o}{I_s}) \frac{\lambda v_{mp}}{(1 + \lambda v_{mp})} \frac{q v_{mp} I_s}{V_B I_B} \qquad (10)$$

Equation (10) can be simplified if electron amplification 'm' is introduced according to

$$I_s = m I_B \qquad (11)$$

which means that a primary particle generates 'm' electron hole pairs

in the solid. In terms of the energy of the electrons V_B, and the average energy expended in creating an electron hole pair ϵ (ionization potential)

$$m = \left(\frac{V_B}{\epsilon}\right) \tag{12}$$

and it can be related to the energy of the gap E_G by the equation

$$\epsilon = f E_G \tag{13}$$

where $f \geqslant 1$. The actual value of 'f' varies in different semiconductors. McKay [8] reports $f = 1.7$ for diamond, [9] $f = 3.2$ for Si and $f = 4.1$ for Ge.

Substituting these relations into equation (10)

$$\eta_{max} = \left(1 + \frac{I_o}{I_s}\right) \frac{\lambda v_{mp}}{(1 + \lambda v_{mp})} \frac{q v_{mp}}{f E_G} \tag{14}$$

From equation (7) it is evident that, if $\frac{I_s}{I_o} > 1$, $\lambda v_{mp} > 1$

and

$$\eta_{max} \cong \frac{q v_{mp}}{f E_G} \tag{15}$$

This relation shows that for large values of V_{max} the maximum efficiency approaches the ratio of the voltage at which electrons are delivered to the load to the average energy spent in freeing an electron hole pair. It implies that most of the liberated electrons flow through the load. This can be shown from equation (8) which shows that if $\lambda v_{mp} > 1$, i_{mp} approaches I_s. Furthermore, equation (7) shows that if $\lambda V_{mp} \gg 1$, $V_{mp} \simeq V_{max}$. For the operating point 'o', the rectangular area i_{mp} times V_{mp} gives power delivered to R_L while remaining area under i-v curve

represents the power lost in the junction.

To establish how E_G affects η_{max}, it is necessary to determine, how the ratio $\frac{I_s}{I_o}$ depends on E_G. The relation between I_s and E_G is given by combining the equations (11), (12), (13)

$$I_s = m I_B \qquad (11)$$

$$m = \frac{V_B}{\epsilon} \qquad (12)$$

$$\epsilon = f E_G \qquad (13)$$

$$I_s = \frac{V_B I_B}{\epsilon E_G} \qquad (16)$$

The dependence of I_o on E_G and other semiconducting parameters as derived by Shockley is given by [10]

$$I_o = \frac{b}{(1+b)^2} \frac{\sigma_i^2}{\lambda} \left(\frac{1}{\sigma_n L_p} + \frac{1}{\sigma_p L_n} \right) = \text{constant} \cdot e^{\frac{-E_G}{KT}} \qquad (17)$$

where b is the mobility ratio, σ_i is the intrinsic conductivity, σ_n and σ_p are the conductivities, L_n and L_p are the minority carrier diffusion lengths of the n and p sides of the junction respectively. It has been found empirically, that I_o does not follow the equation (17), but it can be usually written as

$$I_o = A e^{-\frac{E_G}{BKT}} \qquad (18)$$

where A, the constant depends on the material and B is a constant ≥ 1. If the input flux is large i.e. $\frac{I_s}{I_o} \gg 1$, then $V_{mp} \simeq V_{max}$ and

combining equations (5), (15), (16) and (18), it is found that

$$\eta_{max} = \frac{1}{B f} - \frac{\ln\left(\frac{A_f E_G}{I_B V_B}\right)}{\lambda f E_G} \qquad (19)$$

The second term decreases as E_G increases, so that there is an advantage gained by using a semiconductor with large E_G. The importance of low B and f are evident from the equation (19). They determine the limiting values of η_{max} .

3.2.1 Computation of I_s :

To compute I_s, it is necessary to consider all the possible losses of potential carriers. They are as follows:

(a) Transmission of some of these carriers through the semiconductor .

(b) Reflection losses.

(c) The loss of minority carriers by recombination within the semiconductor before they arrive at the junction.

When all these factors are considered, the expression for I_s assumes the form

$$I_s = Q\,(1 - e^{-\alpha l})\,(1 - r)\,\left(\frac{V_B I_B}{\epsilon}\right) \qquad (20)$$

where Q is the collection efficiency defined as the ratio of the rate of carrier flow across the junction to the total rate of carrier generation in

the solid

r is the reflection coefficient for the electrons

α is the absorption coefficient for the electrons in the solid.

l is the thickness of the absorbing semiconductor.

In deriving the above expression the following assumption was made.

In their passage through matter, electrons are attenuated according to the relation [4(a)]

$$I_B(x) = I_B(o)\, e^{-\alpha x}$$

where $I_B(x)$ and $I_B(o)$ are the electron currents at x and x=o.

3.3. Computation of I_s and Q from the Plane Geometry of the p-n junction:

I_s and Q can be computed from the plane geometry of the cells. The following assumptions were made during the analysis.

1) Since the carrier distribution in the 'p' region is not known, it is convenient to assume that the "p" region is homogeneous and extrinsic.

2) Carrier trapping is negligible. The decay of the excess carriers in the bulk can be characterized by a single exponential i.e. $e^{-t/\tau}$.

3) Conductivity modulation is neglected. ie. The minority carrier density generated by the incident electrons is assumed to be much smaller than the majority carrier density.

Consider the case of an infinite plane p-n junction at x = w with the n region, extending from w to l is as shown in Figure (11). The p region extends from o to w.

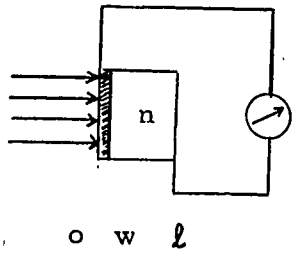

Fig. (11)

3.3.1 Photo Current due to Electrons:

In the 'p' region, the continuity equation for the excess minority carrier density is, assuming unidimensional theory[10]

$$\frac{\partial n'}{\partial t} = \frac{-n'}{\tau_n} + \frac{1}{q} \frac{\partial J_n}{\partial x} + g \qquad (21)$$

where the first term on the right hand side denotes the recombination rate of minority carriers in excess of the equilibrium density np, the second term, the diffusion rate, and the last term is the generation rate due to the incident electrons

$$g(x)\,dx = a N_o e^{-ax}\,dx; \qquad N_o = m\ N_2^* \text{-----21 (a)}$$

where N_2^* is the number of electrons irradiating the surface of the semiconductor at x = o. per second. The current flow from right to left is given by the transport equation.

$$J_n = qD_n \frac{dn'}{dx} \qquad (22)$$

Such a one dimensional model is [11] satisfactory for the photovoltaic cell since the length and width dimensions are large compared with diffusion lengths of minority carriers, Thus surface effects on the edges of the cell can be neglected,

because the assumption that such a cell is sufficiently uniform over its whole area is justified. Only the steady state case is of interest for photovoltaic conversion. Thus equation (21) can be written as

$$D_n \frac{d^2 n'}{dx^2} - \frac{n'}{\tau_n} + \alpha N_o e^{-\alpha x} = o \qquad (23)$$

Since the thickness of the p layer is small (about 1 micron) with respect to the diffusion length of the electrons, the recombination term in equation (23) can be neglected. A constant irradiation level is assumed so that N_o, α are constants. Thus equation (23) becomes

$$D_n \frac{d^2 n'}{dx^2} + N_o \alpha e^{-\alpha x} = 0 \qquad (24)$$

The solution of this differential equation is

$$n'(x) = - \frac{N_o}{\alpha D_n} e^{-\alpha x} + C_1 x + C_2 \quad \text{where} \qquad (25)$$

C_1 and C_2 are constants to be determined from the following set of boundary conditions in the base i.e at $x = o$ and $x = w$. If the contact to the base is a perfect ohmic contact, no minority carriers are injected into or extracted from the base and the only minority carriers lost are those which recombine at the surface of the p layer.

$$s_n [n'(o)] = D_n \left. \frac{dn}{dx} \right|_{x=o} \qquad (26)$$

where s_n is surface recombination velocity

x and $n'(o)$ is the excess concentration at $x = o$.

2) At $x = w$ is the p-n junction which is kept in the zero bias condition, so that a perfect sink for minority carriers exists.

$$n'(w) = p'(w) = 0 \tag{27}$$

Application of these boundary conditions (6) & (7) to (5) gives an expression for n

$$n'(x) = -\frac{N_o}{\alpha D_n}(e^{-\alpha x} - e^{-\alpha w}) - \frac{N_o}{D_n}(x-w) + \frac{s_n[n(o)]}{D_n}(x-w) \tag{28}$$

$n'(o)$ can be found from equation (8) by substituting $x = o$

$$n'(o)\left[1 + \frac{sw}{D_n}\right] = -\frac{N_o}{\alpha D_n}(1-e^{-\alpha w}) + \frac{N_o}{D_n} w \tag{29}$$

The electron current entering the p-n junction

$$= J_n'(x)\Big|_{x=w}$$

$$= q D_n \frac{d_{n'}}{dx}\Big|_{x=w}$$

$$= -q_{N_o}\left[\frac{\alpha w(1-e^{-\alpha w}) - (\frac{sw}{D_n})(\alpha w)e^{-\alpha w} + (\frac{sw}{D_n})(1-e^{-\alpha w})}{\alpha w(1+\frac{sw}{D_n})}\right] \tag{30}$$

This equation represents the increase in diode junction current which is produced by the electron irradiation. This function can be described completely in terms of dimensionless parameters αw, & $\frac{sw}{D_n}$. The parameter αw may be interpreted as the ratio of the base width to the mean depth of penetration $1/\alpha$ of the incident radiation. The parameter $\frac{sw}{D_n}$ is associated with carrier loss by

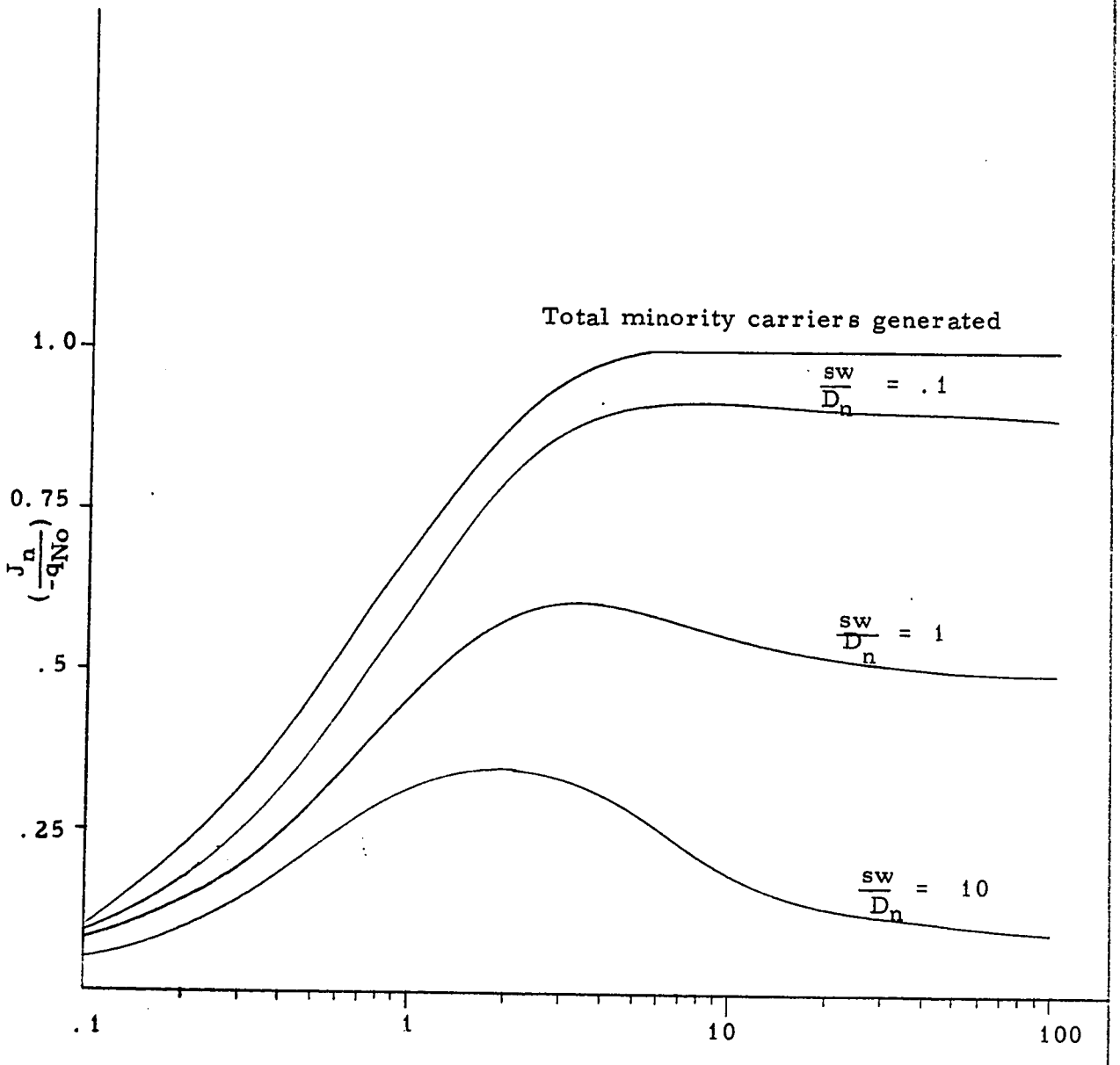

Fig 12: Dimensionless parameter aw versus dimensionless photocurrent.

surface recombination. Dimensionless relative photocurrent versus dimensionless absorption parameter αw for various values $\frac{sw}{D_n}$ were plotted as shown in Figure (12) .

From Figure 12 it can be seen that, for low values of αw, that is for very penetrating radiation, (for very high energy electrons) the increase in diode junction current is very small. The reason is that, at these values of αw, the p layer becomes almost transparent and very few minority carriers are created in the base region. For this kind of radiation the hole current created in the n region and collected by the p layer has to be considered. For nonpenetrating radiation i.e for low energy electrons, most of the electrons are absorbed in the base region and most of the electron hole pairs are created in it.

Next, the effect of the surface recombination velocity upon photocurrent is considered. Dimensionless relative photocurrent vs dimensionless surface recombination losses for low energy electrons were plotted as shown in Figure (13). An increase in $(\frac{sw}{D_n})$ i.e. increase in the recombination rate at the surface, decreases the electron photocurrent, since more minority carriers are lost on the surface and will not reach the junction, as is evident from Figure (13). For very large αw, most of the electrons are absorbed in a thin layer just beneath the surface and thus many minority carriers are lost by the surface recombination and do not contribute to the electron photocurrent. This explains the decrease of the curves in Figure (12) for very large values of αw when the recombination parameter is comparatively large.

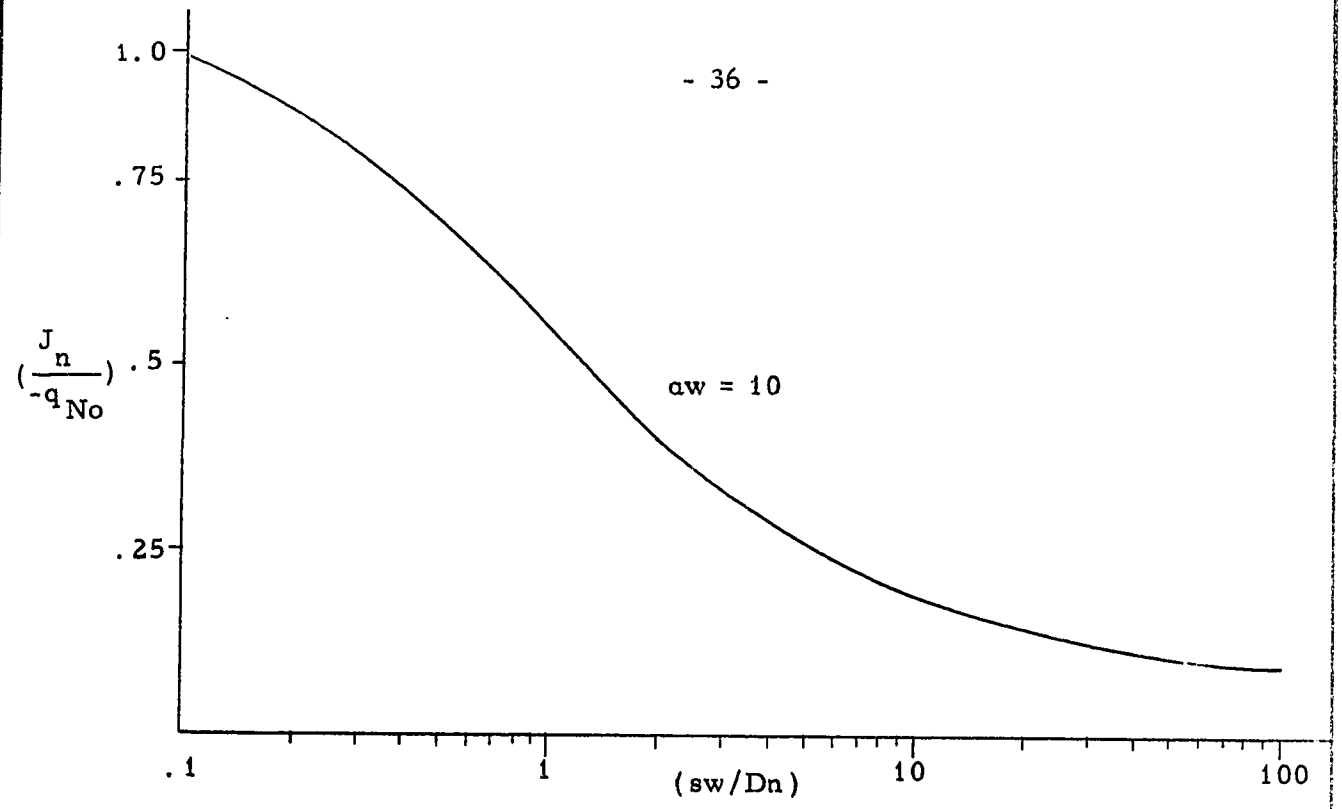

Fig. (13) Dimensionless surface recombination loss versus dimensionless photocurrent.

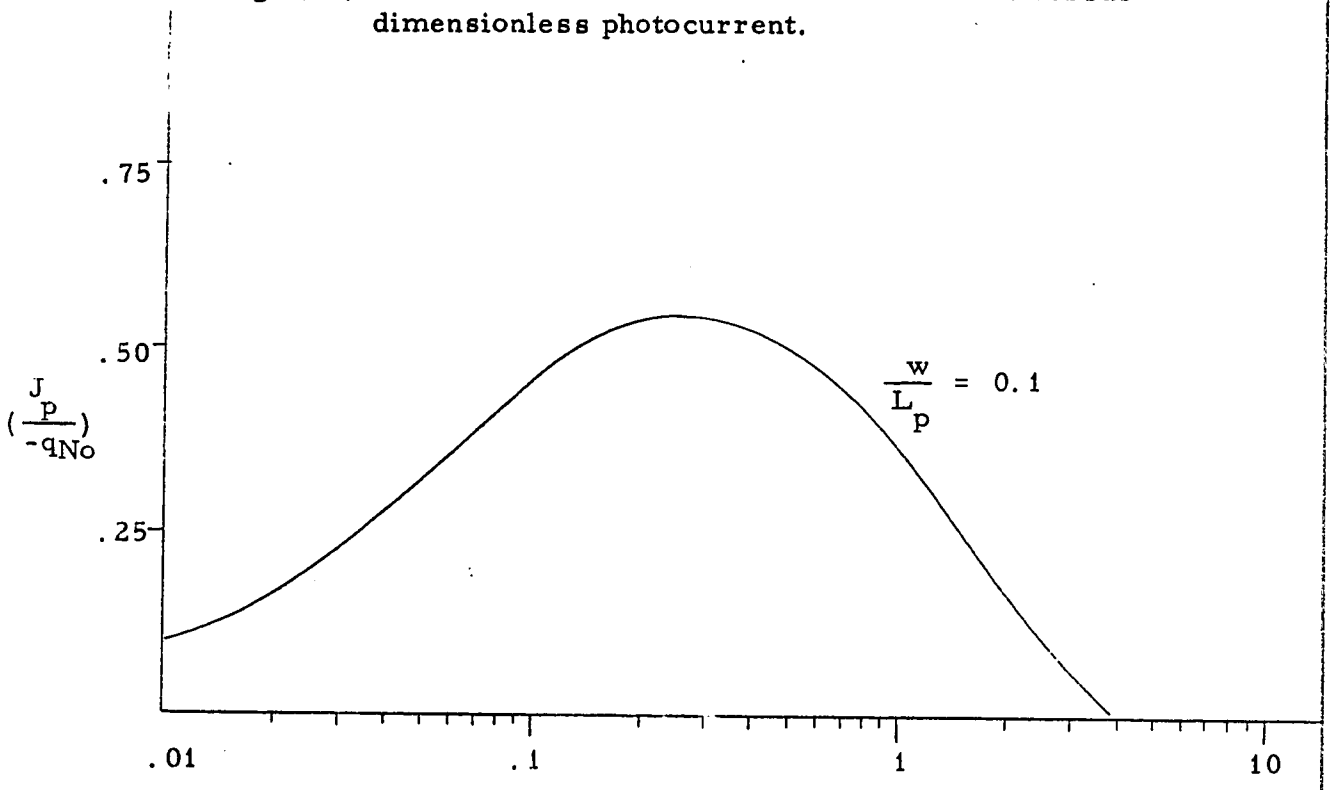

Fig. (15) Dimensionless parameter αw versus dimension - less photocurrent.

3.3.2 The Hole Current through the Diode:

The n region of the cell has some effect on the overall photocurrent of the diode, since excess minority carriers (holes) are absorbed by the high energy electrons which has not been absorbed in the p layer.

To account for the hole contribution to the overall current of the cell, the differential equation for the minority carriers in the n region must be solved. Since the depletion layer is quite thin, the photogeneration in the space charge layer can be neglected. The n region can be taken from x = w as shown in Fig. (14).

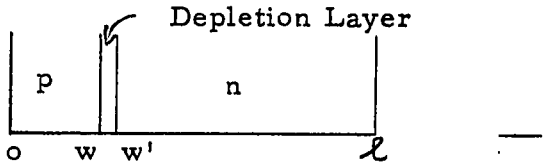

Fig. (14)

The continuity equation for $x > w$ is

$$\frac{\partial p'}{\partial t} = -\frac{p'}{\tau_p} - \frac{1}{q}\frac{\partial J_p}{\partial x} + g \qquad (31)$$

where the first term on right hand side denotes the recombination rate of minority carriers in excess of equilibrium density p_n, the second term is diffusion rate and the last term is the generation rate.
The current flow from left to right is given by

$$J_p = -qD_p \frac{dp'}{dx} \qquad (32)$$

Equation (11) becomes

$$D_p \frac{d^2 p'}{dx^2} - \frac{p'}{\tau_p} = - a N_o e^{-ax} \qquad (33)$$

The solution is

$$p'(x) = Ae^{x/L_p} - \frac{a N_o e^{-ax}}{D_p(a^2 - \frac{1}{L_p^2})} + Be^{-x/L_p} \qquad (a \neq \frac{1}{L_p}) \qquad (34)$$

where A and B are constants to be determined from the following set of boundary conditions

$$p'(x)\Big|_w = 0$$

i.e at $x = w$ the excess hole concentration is negligible since the minority carriers are swept out by the depletion layer.

At $x = \ell$ assuming that there is a perfect ohmic contact, no excess minority carriers are injected into or extracted from the bulk.

$$p'(x = \ell) = 0$$

The hole current flowing through the diode $= J_p(x)\Big|_w = q D_p \frac{dp'}{dx}\Big|_{x=w}$

Equation (34) is solved with the above boundary values and solving for $J_p(w)$, we get

$$J_p(w) = - qN_o \left[\frac{(aw)^2 e^{-aw}}{(aw)^2 - (\frac{w}{L_p})^2}\right] + \frac{w(aw)}{L_p[(aw)^2 - (\frac{w}{L_p})^2]e^{a\ell}} \sinh(\frac{\ell - w}{L_p})$$

$$- \frac{w(aw)e^{-aw}\coth(\frac{\ell - w}{L_p})}{L_p[(aw)^2 - (\frac{w}{L_p})^2]}$$

If $\ell > L_p$ then the above equation reduces to

$$J_p(w) = - qN_o \left[\frac{aw\, e^{-aw}}{(aw + \frac{w}{L_p})}\right] \qquad (35)$$

Equation (35) is plotted as shown in Figure 15. As mentioned above, the photocurrent depends on the particular type of radiation used. i.e on the energy of the incident electrons. For large values of αw i.e for low energy electrons, only the electron current has to be considered since the hole current is negligible as is evident from Figure 15. Alternatively for penetrating radiation, the photocurrent due to electrons becomes less important and the hole current contributes most of the current. That is for very penetrating radiation, the photocurrent depends on the 'n' region and the thickness of the 'p' region. Now the total current passing through the junction is equal to the sum of the electron and hole currents [equation (10) & (15)]. The collection efficiency

$$Q = \frac{\text{Total current passing through the junction}}{\text{Total minority carrier current generated}}$$

$$= \frac{J_n(w) + J_p(w)}{N_o (1 - e^{-\alpha \ell})} \qquad (36)$$

If ℓ is large with respect to the range of the electrons the denominator becomes N_o.

3.4 Photo Diode Mode:

When a reverse bias is applied to a photovoltaic cell, it is called photodiode. If the diode is irradiated by an electron beam the reverse current increases proportionally to the incident radiation as a result of the extra carriers introduced in the semiconductor material by the absorbed electrons. The equivalent circuit diagram of the photodiode is given in Figure (16)[4]b .

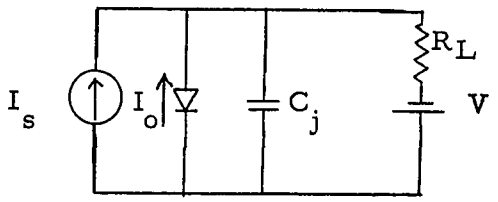

Figure (16): Equivalent circuit diagram for photodiode.

I_s is the photocurrent generated due to the absorption of the electrons. I_o is the junction current of the diode which is equal to reverse saturation current. C_j is the transition region capacitance. In the photodiode operation the junction is reverse biased and thus the current through the junction is in the same direction as the current from the photocurrent generator.

The sensitivity of the photodiode is generally measured against dark current. Important for a good photodiode are high reverse voltages in order to obtain high gain, low dark currents for good sensitivity. The photocurrent can be evaluated theoretically from the plane geometry of the cell. In the present case, the total photocurrent consists the following.

1) Photocurrent generated in the 'p' region
2) Photocarrier generation in the space charge region
3) Photo current generated in the 'n' region.

3.4.1 Photocurrent due to Electrons:

In the 'p' region, the continuity equation for the minority carrier density is, assuming unidimensional theory[10],

$$\frac{\partial n}{\partial t} = \left(\frac{np-n}{\tau_n}\right) + \frac{1}{q}\frac{\partial J_n}{\partial x} + g \qquad (37)$$

The first term on the right hand side of equation (37) denotes the recombination rate of minority carriers, the second term is the diffusion rate and the last term is the generation rate due to the incident electrons.

As in the photovoltaic case the steady state equation can be solved with the following boundary conditions.

1) At $x = w$ $p(w) = 0$ since at $x = w$ for reverse voltages much higher than $\frac{KT}{q}$ the electron concentration is negligible.

$$p = p_n e^{\frac{qv}{KT}} \quad \text{if} \quad |v| \gg \frac{KT}{q}, \; v \text{ is negative}$$

$$p = 0$$

2) At $x = 0$ $\quad s_n(n-np)_{x=o} = D_n \left.\frac{dn}{dx}\right|_{x=o}$

where s_n is the surface recombination velocity for electrons. The electron current entering the depletion layer

$$J_n = q D_n \left.\frac{dn}{dx}\right|_{x=w} \text{ --- (22)}$$

Solving equation (37) with the above boundary conditions and evaluating equation (22), we get

$$J_n = -qN_o \left[\frac{\alpha w(1-e^{-\alpha w}) - \frac{sw}{D_n}(\alpha w)e^{-\alpha w} + \frac{sw}{D_n}(1-e^{-\alpha w})}{\alpha w(1 + \frac{sw}{D_n})} \right] - \frac{q(sn_p)}{(1 + \frac{sw}{D_n})} \qquad (38)$$

where the first term denotes the photocurrent, the second term denotes dark current.

The first expression shows that the photocurrent is independent of the applied voltage. This is, because of the first boundary condition, which applies for reverse bias voltages several times higher than $(\frac{KT}{q})$. For voltages comparable to $(\frac{KT}{q})$, the minority carrier concentration at x = w is not zero, but it depends on the voltage drop across the junction and thus on the applied voltage.

In the above analysis the part of the 'p' region which is inside the space charge region is disregarded and the effective 'p' region ends at x = w as shown in Figure (17).

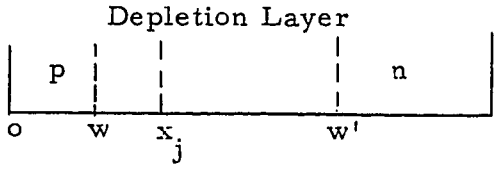

Figure (17)

Where (w' - w) is the width of the depletion layer, (w'-xj) on 'n' side and (xj-w) on p side of the junction. The first expression in equation (38) is similar to the photovoltaic case.

3.4.2 Photogeneration in the Depletion Region:

The photogeneration in the space charge region cannot be neglected if the range of the incident electrons within the bulk of the semiconductor is not large. The steady state continuity equation for the minority carrier density in the space charge region is for $x > xj$ (Figure 17)

$$- \frac{p}{\tau_p} - \mu \frac{\partial}{\partial x} (E\, p) + \alpha N_o e^{-\alpha x} = 0 \qquad (39)$$

In the above equation diffusion term is neglected when compared with drift term. In equation (39), the first term denotes recombination of the minority carriers, second and third terms denote drift rate and generation rate respectively, where E is the electric field and the other parameters involved in equation (39) are mentioned in the earlier sections.

The relationship between the electric field, voltage, and space charge widening can be found by solving the Poisson's Equation

$$\frac{d^2v}{dx^2} = - (N_d - N_a) \left(\frac{4\pi q}{e} \right) \qquad (40)$$

In the above equation it is assumed that all the atoms are ionized.

where v is the voltage

q is the electronic charge

e is the permittivity of the material.

N_d and N_a are the number of donor and acceptor impurity sites within the space charge region. Assuming 'p' layer is heavily doped, then the whole depletion layer lies within the 'n' region. Since 'p' layer is heavily doped the diffused junction is assumed as an abrupt junction. The poisson's equation for $x > x_j$ is

$$\frac{d^2v}{dx^2} = - N_d \left(\frac{4\pi q}{e} \right) = \frac{dE}{dx} = K \quad \text{(say)} \qquad (41)$$

The solution of this differential equation is

$$E = (Kx + c_1) \qquad (42)$$

where c_1 is a constant which can be determined from the following boundary condition.

At $x = w^1$ $\quad E = 0$.

This is because the absolute values of the charge on one side of the junction must be equal to that of the other side. Since there is no charge outside the space charge region, E must be zero at both edges of the space charge region and at $x = x_j$, E is maximum .

$$\text{Therefore } E = K(x - w^1) \tag{43}$$

Equation (39) becomes

$$\mu K(x-w^1) \frac{dp}{dx} + p(\mu k + \frac{1}{\tau_p}) = \alpha N_o e^{-\alpha x} \tag{44}$$

For typical values of μ, K, and τ_p for an extrinsic semiconductor, it is found that $\frac{1}{\mu k \tau_p} << 1$, which is verified as follows:

Assuming $\mu = 15 \times 10^4$ cm^2/strat Volt sec

$q = 4.8 \times 10^{-10}$ es.u

$\tau_p = 1$ to 10 μ sec

$N_d = 10^{17}$ atoms /c.c.

$e = 12$ for Si

Substituting these values, it is found that

$$\frac{1}{\mu k \tau_p} << 1$$

Solving equation (44) for p, we obtain

$$p(x) = - \frac{1}{\mu k(x-w^1)} [N_o e^{-\alpha x} + c_2] \tag{45}$$

where c_2 is a constant and is determined from the following boundary condition.

$$\text{At } x = w^1 \quad p(w^1) = 0 \tag{46}$$

Substituting equation (46) in (45),

$$p(x) = - \frac{N_o}{\mu k(x-w^1)} [e^{-\alpha x} - e^{-\alpha w^1}] \tag{47}$$

Equation (47) gives the minority carrier density generated due to the incident electrons. Figure (18) shows the variation of the photocarriers generated, in the presence of radiation and in the absence of radiation.

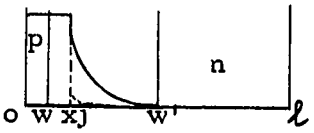

—— Photocurrent in the presence of incident radiation

-----Current in the absence of radiation

Figure (18)

The hole current flowing into the 'p' region

$$= \mu E p \Big|_{x=x_j} \tag{48}$$

$$= - qN_o \left[e^{-\alpha x_j} - e^{-\alpha w^1}\right] \tag{49}$$

The width of the depletion layer can be determined from the type of the junction for a given reverse bias voltage.[10] The total minority carriers generated within the depletion layer is $N_o(e^{-\alpha w} - e^{-\alpha w^1})$. Thus the collection efficiency within the depletion layer is approximately 100%. So by proper reverse bias, it is possible to stop the incident electrons, within the depletion layer and thus obtain a high collection efficiency.

3.4.3: Hole Current Through the Diode

If the incident electrons are absorbed beyond the depletion layer, then the 'n' region of the diode can have some feffect on the overall photocurrent. The steady state continuity equation for $x > w^1$ is (Figure 17)

$$\left(\frac{p_n - p}{\tau_p}\right) - \frac{1}{q} \frac{\partial J_p}{\partial x} + g = 0 \tag{50}$$

The first term in equation (50) denotes the recombination rate of minority carriers (holes), the second and third term denote diffusion rate of holes and generation rate due to the incident electrons. The above differential equation is solved with the following boundary conditions

1) At $x = w^1$ $\quad p(w^1) = 0$ since at $x = w^1$, reverse voltages much higher than $\frac{KT}{q}$, the hole concentration is zero.

2) Assuming $\ell >> L_p$, at $x \to \infty$ $p(x)_{\infty} = p_n$

The hole current entering the depletion layer

$$J_p = - q D_p \left.\frac{dp}{dx}\right|_{x=w^1}$$

Solving equation (50) with the above boundary conditions and evaluating J_p, it gives

$$J_p = -q N_o \left[\frac{\alpha w^1 e^{-\alpha w^1}}{\alpha w^1 + \frac{w^1}{L_p}}\right] - \frac{q p_n D_p}{L_p} \qquad (51)$$

The first term in equation (51) denotes photocurrent and the second term denotes dark current. If the range of the incident electrons is large i.e. several times greater than the depletion layer, the photogeneration in the space charge region can be neglected. And in equation (51) w^1 can be replaced by w. Thus hole current flowing through the diode is given by

$$J_p = - q N_o \left[\frac{(\alpha w)\, e^{-\alpha w}}{\alpha w + \frac{w}{L_p}}\right] \qquad (52)$$

As explained in section 3.3.2, the whole photocurrent is contributed by holes for very penetrating radiation, the above equation gives the total photocurrent.

3.5: Radiation Damage:

Radiation damage [12] by high energy electrons limits the life of the cells. The damage process appears to be the production of Frenkel defects by high energy electrons. Such defects act as bulk recombination centres and reduces the minority carrier life time. Radiation damage reduce the cell efficiency primarily by causing recombination of the added carriers before they can diffuse to the junction. Radiation damage does not occur below the threshold energy E_t, which is about 325 Kev for Ge and 145 Kev for Silicon.

3.6: Effect of Temperature:

The theory of the photovoltaic effect shows the highest efficiency is realized when the rate of generation of carriers is much higher than the rate of thermal generation. This rate falls rapidly as the temperature increases, so the output decreases.

3. Review of Known Experimental Results:

Rappaport [4a] et. al obtained current amplification ratio m, and the ionization potential 'ϵ' by using an electron gun source. ('m' and 'ϵ' are defined in section 3.2.). The following table lists the values of m and 'ϵ' for various values of beam voltages(V_B).

V_B	m	ϵ
50 Kev	8.8×10^3	5.7 eV
80 Kev	1.9×10^4	4.3 ev
100 Kev	1.9×10^4	5.3 ev

It is evident from the table, that for the values of V_B used there is no significant variation in ϵ.

Ehrenberg and his Coworkers [14] obtained a current gain of 500, when Se photocells were bombarded by 50 Kev electron beam.

Rappaport [15] measured the electron voltaic effect resulting from the bombardment of an alloy typed p-n junction with β particles. The wafers used were not more than one diffusion length thick. The voltage and current, which such a device exhibited is similar to that arising from a photovoltaic cell except in the present case, the carriers are produced throughout the volume of the semiconductor. Current gain of several thousands was obtained after corrections for surface recombination velocity etc. were made.

Kimoto [15] and his Coworkers obtained a current gain of 2500 when they bombarded, a p-n diffused junction with a 25 Kev electron beam.

Takeja et. al [16] obtained current gains of several hundreds with different cells in photodiode mode.

CHAPTER 4

EXPERIMENTAL VERIFICATION

This investigation was carried out on the behaviour of Si p-n junctions and Au-Si thin film contact under low energy electron bombardment (10 Kev) in photovoltaic and photodiode modes. As mentioned previously the very high energy electrons (threshold energy for Si .145 Mev) cannot be used for the current multiplication, because of the formation of Frenkel defects. Electrons of low and medium energy can be used for this purpose.

4.1 Devices investigated:

Large area (.25 sq cm) diffused type p-n junctions were made by diffusing boron atoms into n type silicon. The thickness of the 'p' region is of the order of 1 to 2 microns. The resistivity of the semiconductor was chosen as low as possible consistent with high life time so that potential barrier was high and therefore dark current was low. The dark current of these cells is of the order of 1 μA. The resistivity of the wafers is in the range of 1 to 5 ohm cm. Gold-silicon thin film contact was made by evaporating gold film of about 100°A thick on n type silicon. It has an effective area .25 sq cm. The dark current of this cell is about 10^{-7} amps. Figure (19 shows the experimental arrangement used for bombarding the cells.

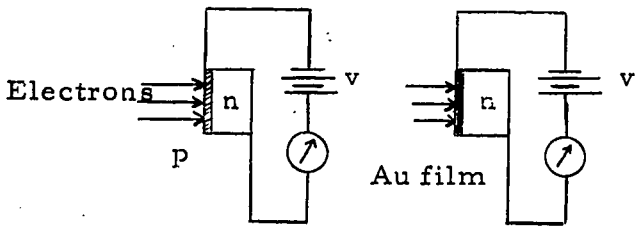

Figure (19

The 'p' layer of the diode is bombarded by electrons. This layer is called the base layer of the diode. As a result of the bombardment electron hole pairs are produced in the base, the space charge region, and in the bulk of the diode depending upon the intensity of irradiation. The inequilibrium minority carriers i.e. electrons from the p region moving towards the p-n junction will be captured by the field and leave the junction. Similarly holes from 'n' region pass through the p-n junction and leave the junction. The increase of reverse current caused by the incident electrons, exceeds the magnitude of the irradiation current since the formation energy of an electron hole pair is about 3.7 ev for Si, denoting the increase of current in the reverse direction by $\Delta r_{ev} = (I_2 - I_o)$ where I_2 is the reverse current in the presence of radiation and I_o is the reverse current in the absence of radiation i.e dark current of the diode.

I_B is the magnitude of the irradiation current, then the quantity $m = \frac{\Delta_{rev}}{I_B} \simeq \frac{I_2}{I_B}$ (if $I_2 > I_o$) can be considered as the amplification factor.

4.2 Description of the Apparatus:

Two cells A and B are mounted symmetrically on circular copper plate which is supported on the base plate of the bell jar as shown in Figure (20). The two cells are isolated from the copper plate. The electrical connections are taken from the feed throughs of the vacuum chamber. The filament is placed normal

to the plane of the cells as shown in Figure (20). The filament connections are shown as shown in Figure (20).

The electrons that are emitted from the filament are accelerated towards the cells by applying negative voltage between the filament and the ground as shown in Figure (20). To limit the load on the high voltage power supply, the unit is shielded from the rest of the vacuum system by enclosing it in a cylindrical copper mesh, connected to the cathode.

In Figure (20), cell 'A' represents Si p-n diode and cell B is a thin copper plate of $^{7}/_{8}$" diameter. This arrangement permits the measurement of the electron flux falling on the standard cell and at the same time the increase in diode current due to irradiation. It is assumed that the electron flux incident on the cells is equal, because of the symmetry of the arrangement. This approximation is fairly accurate which was verified. The standard cell is coated with material, having a low back-scattering coefficient such as carbon. The electron flux incident on the standard cell, can be measured as a current by a current meter which is placed between the standard cell and the ground as shown in Figure (20a). The increase in diode current due to photocarriers was measured for various reverse bias voltages as shown in Figure (20b). All the measurements were carried out with continuous evacuation in vacuum of the order of 0.5 to 1 x 10^{-6} torr.

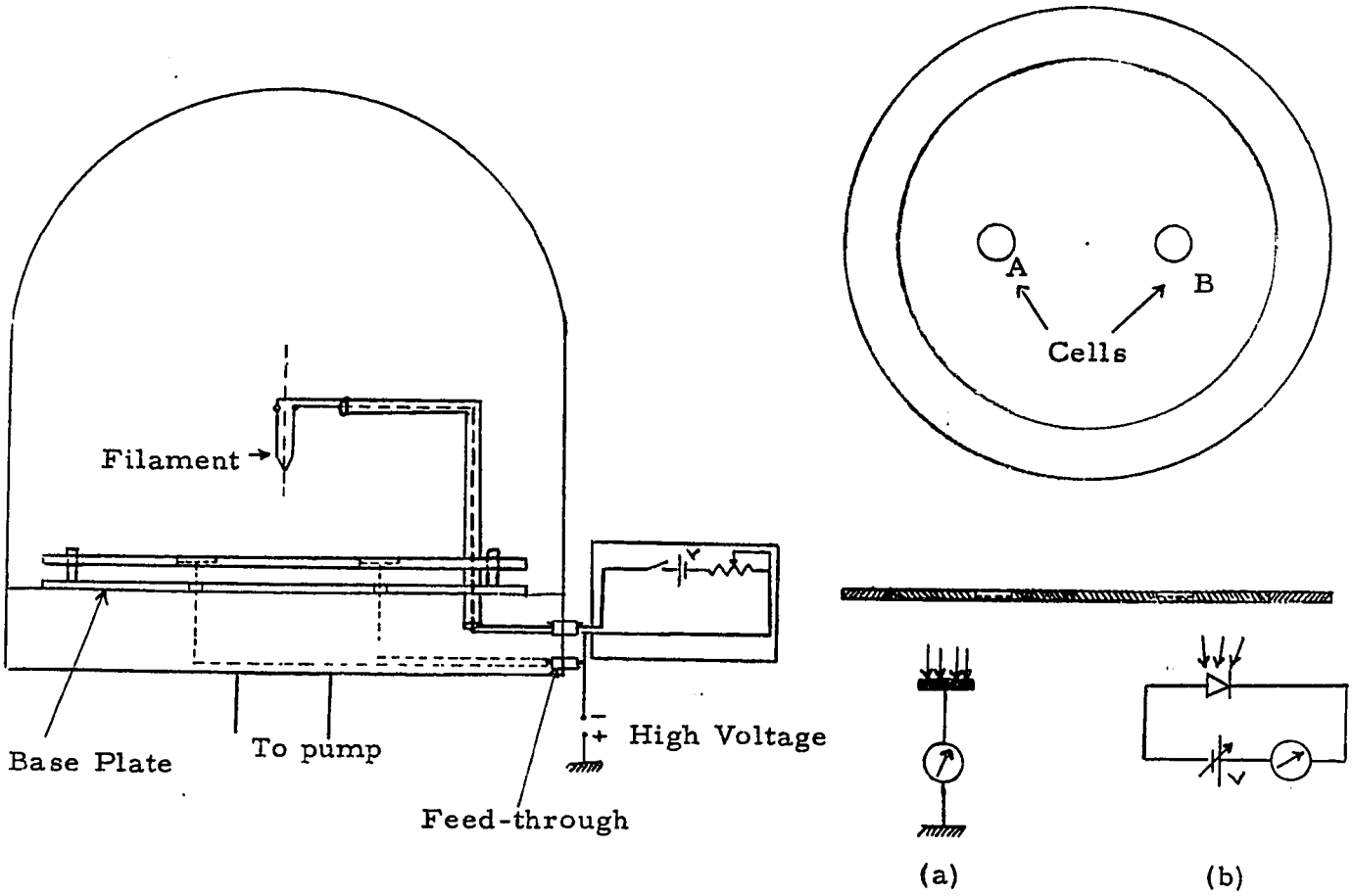

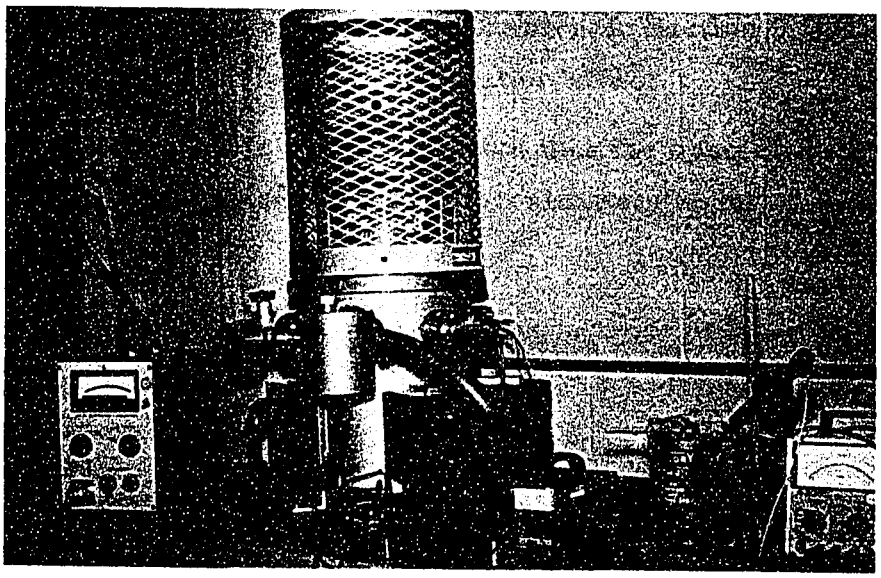

Figure 20 Experimental Set-up and Assembly.

Experimental Results:

For various values of the energy of the bombarding electrons, the electron flux irradiating the cells, the photocurrent, and the open circuit voltage were measured and were given in Table 2. The theoritical values of the open circuit voltage were calculated from equation (5) of Section 3.2 and are tabulated. The dependence of the amplification factor, on the energy of the bombarding electrons is shown in Figure(21).

The amplification factor increases monotonically with increase of the electron energy as is evident from the graph. The shape of this curve depends on the thickness of the base layer and the surface state of silicon. The surface recombination losses are high for very low energy electrons. For low energy electrons, they are absorbed near the surface and the electron hole pairs that are generated are recombined at the surface. Therefore the total current flowing towards the junction is small. By increasing the energy of the electrons, the depth of formation of electron hole pairs increases and substantially decreases the effect of the surface recombination. For sufficiently high energy electrons, the photocurrent is entirely due to holes (n region) as explained in Chapter 3, Section 3.3.2, thus eliminating the surface recombination effect.

From Table (2), it is shown that the open circuit voltages, calculated and measured, are approximately equal.

P-N Junction Cell:

Dark current = 1 μA (I_o)

Bias voltage = ov

Energy of the incident Electrons	Standard Current (I_B)	Photo-current (I_2)	Gain $= \left(\frac{I_2 - I_o}{I_B}\right)$	Open ckt voltage	Theoritical open circuit voltage $V = \frac{1}{\lambda} \ln\left(\frac{I_s}{I_o} + 1\right)$
4.5 kev	1×10^{-8} Amp	3 μA	200	30 mV	35 mV
5.0 kev	"	3.5 μA	250	35 mV	37.5 mV
6.0 kev	"	4.5 μA	350	40 mV	43 mV
7.0 kev	"	6.0 μA	500	45 mV	49 mV
8.0 kev	"	8.0 μA	700	50 mV	55 mV

Table -2

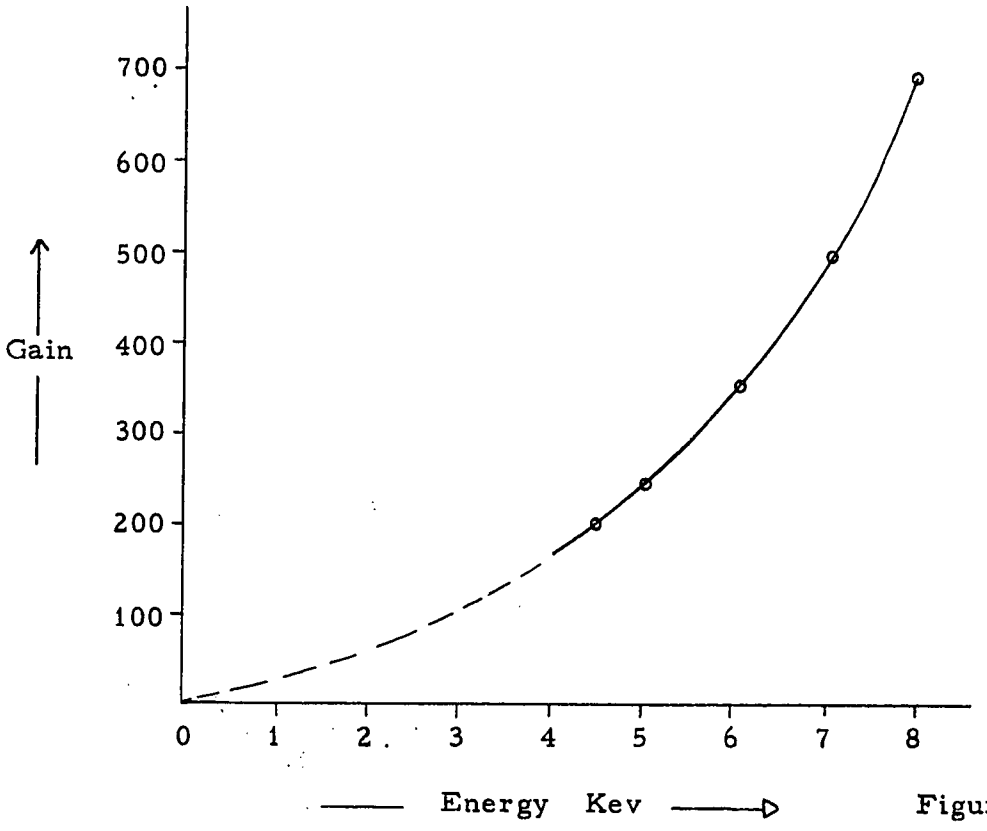

Figure (2)

For various values of the energy of the bombarding electrons, the electron flux irradiating the cells, and the photo-current for various values of bias voltages were measured. The dependence of the amplification factor on the junction voltage was shown in Figure (22). As the bias voltages increases, the gain increases and with further increase in the bias voltage, the gain becomes constant. This is due to the increased potential gradient, which improves the motion of electron-hole pairs in the field towards the junction, and thus improves the collection of all the electron hole pairs. The saturation of the characteristics is observed at 4 v.

Further increase of the junction voltage, leads to an increase of gain as shown in Figure (23). This increase in gain is not connected with the heating of the junction because it is fully reproducible with increase or decrease in voltage. This can be due to the increased potential gradient and the resulting avalanche effect, which increases the number of carriers.

The experiment was repeated with different p-n junction cells and it was observed that the results were consistent within the experimental error as shown in Figure (24).

Similar experiment was carried out on the gold-silicon thin film contact. The dependence of the amplification on the bombarding electrons for various reverse bias voltages was shown in Figure (25).

Cell No 1: Dark current = 1 μA

Si p-n junction cell

Energy of the electrons	Standard Current	Diode Photo Current at 'o' v	- 1v	-2v	-3v	-4v	-5v	-6v
5 Kev	1.7×10^{-8} Amp	3.4μA	4.5μA	7.75μA	9μA	10μA	10μA	10μA
6 Kev	1.7×10^{-8} Amp	6.5μA	8.0μA	10.0μA	12μA	10.75μA	12.75μA	12.75μA
7 Kev	1.7×10^{-8} Amp	9.25μA	11.0μA	12.75μA	14μA	15μA	15μA	15μA
8 Kev	1.7×10^{-8} Amp	12μA	13.5μA	15.25μA	16μA	17μA	17μA	17.25μA

Energy of the electr.	Standard current	Gain at 'o' v	-1v	-2v	-3v	-4v	-5v	-6v
5 Kev	1.7×10^{-8} Amp	200	300	410	530	590	590	590
6 Kev	1.7×10^{-8} Amp	380	470	590	700	750	750	750
7 Kev	1.7×10^{-8} Amp	540	650	750	820	880	880	880
8 Kev	1.7×10^{-8} Amp	700	800	900	950	1000	1000	1010

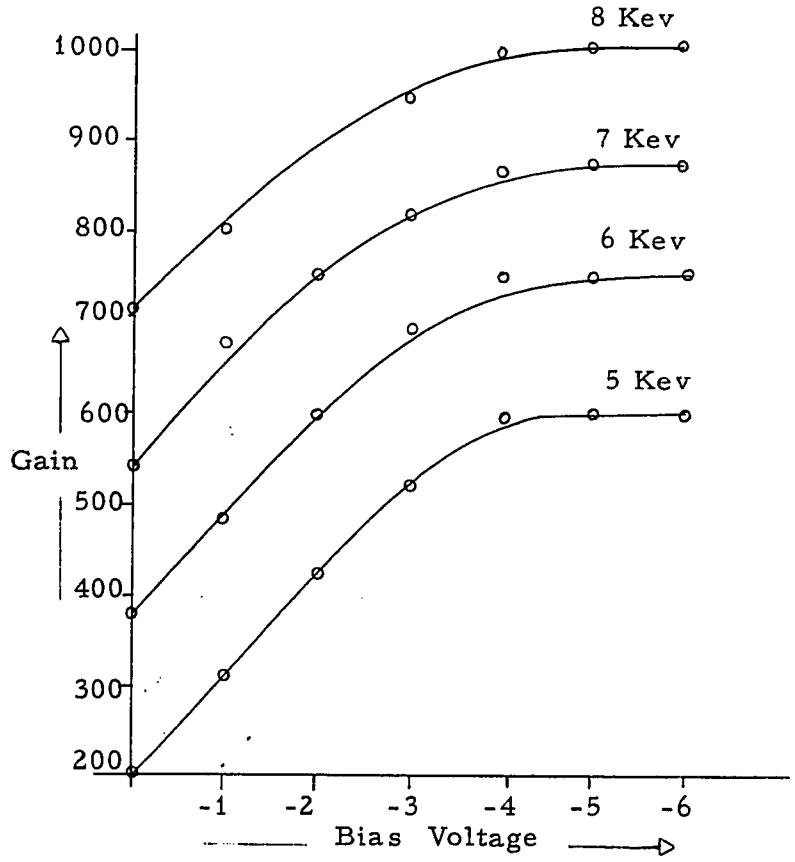

Figure (22)

Cell no 1: Si p-n junction cell

Dark current = 1 μA

Energy of the incident Electrons	Standard current	Diode Photo-current at 'o' v	-1v	-2v	-3v	-4v	-5v	-6v	-7v	-8v
7 Kev	1.7×10^{-8} A	9.25μA	11.0μA	12.75μA	14μA	15μA	15μA	15μA	16μA	17.75μA
8 Kev	1.7×10^{-8} A	12μA	13.5μA	15.25 μA	16μA	17μA	17μA	17.25μA	18.25μA	20.5μA

Energy of the incident Electrons	Standard Current	Gain at 'o'v	-1v	-2v	-3v	-4v	-5v	-6v	-7v	-8v
7 Kev	1.7×10^{-8} A	540	650	750	820	880	880	880	940	1040
8 Kev	1.7×10^{-8} A	700	800	900	950	1000	1000	1010	1090	1210

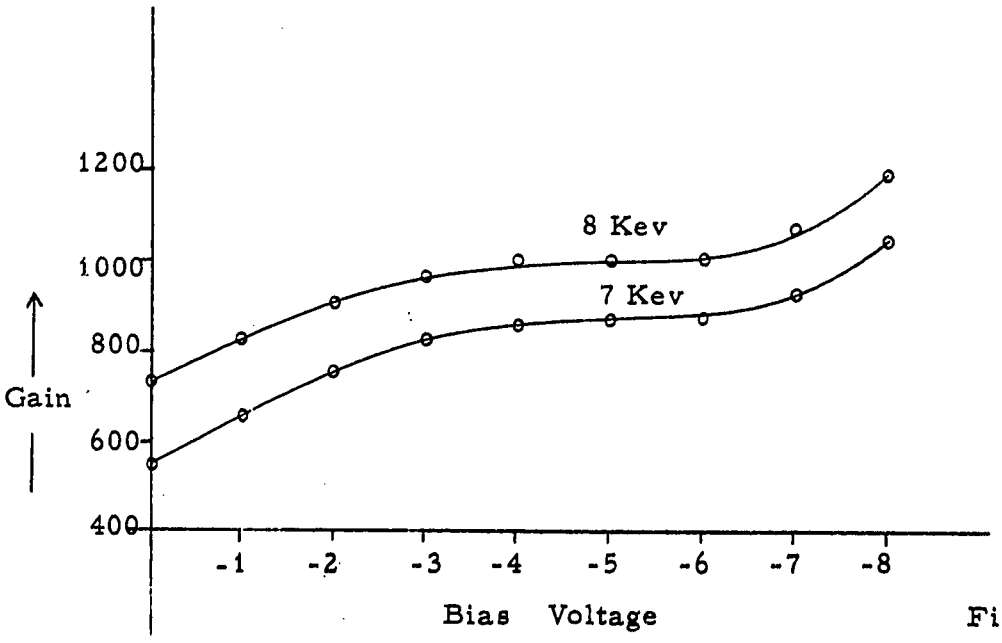

Figure (23)

Cell No 2: Si P-n junction cell

Dark Current = 1μA

Energy of the electrons	Standard Current	Diode Photo Current at 'o' v	-1v	-2v	-3v	-4v	-5v	-6v
5 Kev	$2x10^{-8}$A	4.5μA	6.0μA	8.0μA	10μA	11μA	11μA	11μA
6 Kev	$2x10^{-8}$A	7.5μA	9.5μA	11.0μA	13.0μA	14μA	14μA	14μA
7 Kev	$2x10^{-8}$A	10.5μA	12.5μA	14.0μA	15.5μA	16.5μA	16.5μA	16.5μA
8 Kev	$2x10^{-8}$A	14.0μA	16.0μA	17.5μA	18.5μA	19.5μA	19.5μA	19.5μA

Energy of the electrons	Standard Current	Gain at 'o'v	-1v	-2v	-3v	-4v	-5v	-6v
5 Kev	$2x10^{-8}$A	225	300	400	500	550	550	550
6 Kev	$2x10^{-8}$A	375	475	550	650	700	700	700
7 Kev	$2x10^{-8}$A	525	625	700	775	825	825	825
8 Kev	$2x10^{-8}$A	700	800	875	925	975	975	975

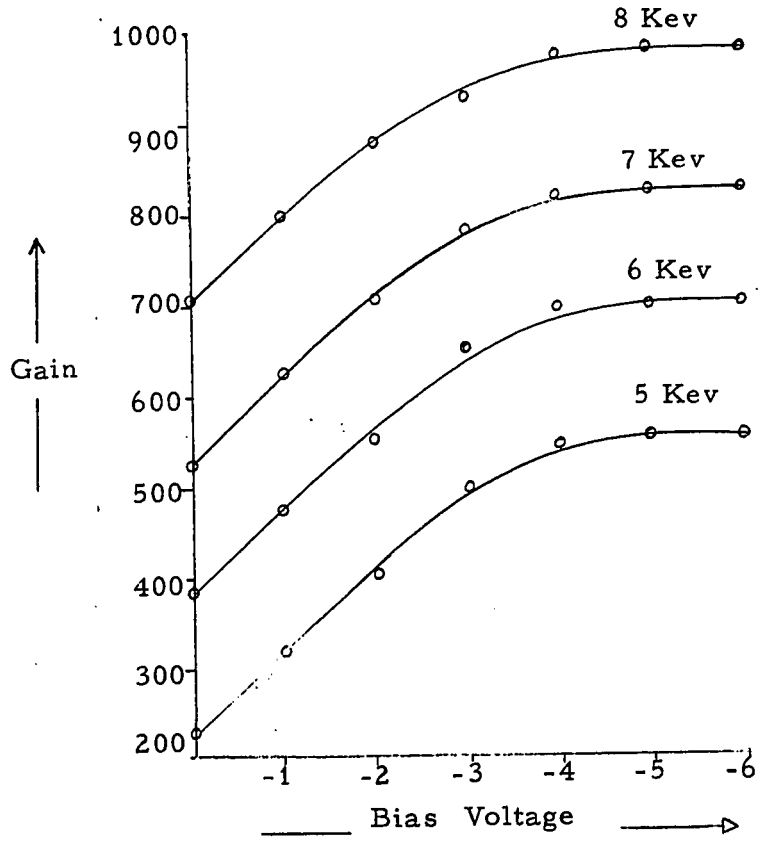

Figure (24)

Au-Si thin film contact

Dark Current = 10^{-7} Amp

Energy of the incident Electrons	Standard Current	Diode photo Current at 'o' v						
5 Kev	$2x10^{-8}$ A	6.5μA	9.0μA	12μA	13.5μA	13.75μA	13.75μA	14 μA
6 Kev	$2x10^{-8}$ A	9.0μA	12.0μA	14μA	15.5μA	16.0μA	16.0μA	16.0μA
7 Kev	$2x10^{-8}$ A	12.0μA	14.0μA	16.5μA	17.5μA	18.0μA	18.0μA	18.0μA

Energy of the incident Electrons	Standard Current	Diode Gain at 'o' v	-2.5v	-5v	-7.5v	-10v	-12.5v	-15v
5 Kev	$2x10^{-8}$ A	325	450	600	680	690	690	700
6 Kev	$2x10^{-8}$ A	450	600	700	780	800	800	800
7 Kev	$2x10^{-8}$ A	600	725	825	875	900	900	900

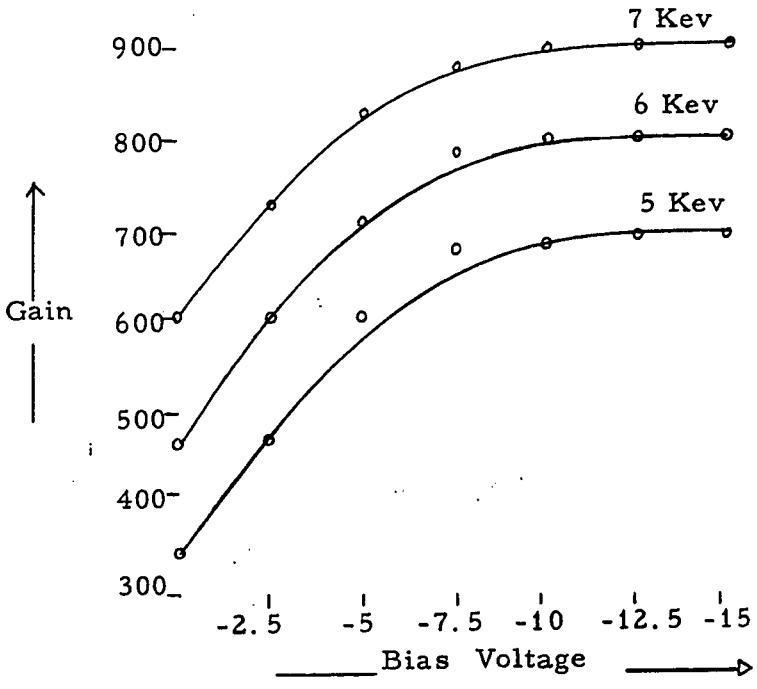

Figure (25)

The ionization energy i.e. the energy spent in freeing an electron hole pair can be calculated from the energy of incident electrons and the amplification factor. It is obtained by dividing the energy of the incident electrons with the amplification factor. The ionization energy and the amplification factor are given in Table (3).

Table (3)

Energy of the incident Electrons	Ionization Energy	Amplification Factor.
5 Kev	8.5 ev	590
6 Kev	8.0 ev	750
7 Kev	8.0 ev	880
8 Kev	7.9 ev	1010

These values are high, compated with the theoretical value (Ionization energy for Si = 3. 7 ev), because of the reflection losses and low collection efficiency. The collection efficiency of the cells is mainly dependent on the surface state of the silicon, and can be found as follows.

Assuming a reflection coefficient for silicon[17] of 20% , the collection efficiency of the cell can be determined by assuming the ionization energy for silicon to be 3.7 ev[8] and the ionization energy from table (3) (8 ev).

Then the collection efficiency of the cell

$$= \frac{\text{Theoretical value of the ionization energy}}{\text{Practical value of the ionization energy x percentage of reflection losses}}$$

$$= \frac{3.7}{8} \times \frac{100}{80} \times 100 = 59\ \% .$$

CHAPTER 5

APPLICATIONS

5.1 Arrangement of Detectors:

As mentioned in Chapter 1, in a scanning electron microscope, either back-scattered or secondary electron image can be viewed on a cathode Ray oscilloscope. Generally reflected electrons are used for the topological and chemical inspection. When finer details are required, the secondary electron image is used[3].

The schematic diagram for obtaining reflected electron image using this cell is shown in Figure (26).

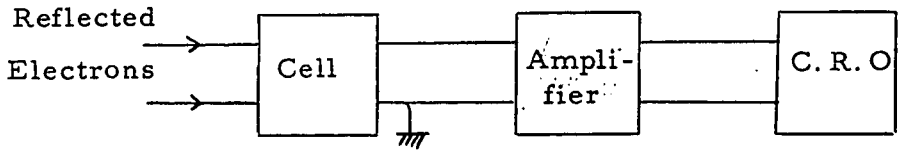

Figure (26)

In a scanning electron microscope, the specimen is at ground potential. Since the reflected electrons possess high energy, acceleration is not necessary and they can straightaway be used for irradiating the cell. As such, the cell can be at the ground potential.

However, the secondary electrons possess very low energy, and need acceleration before using them for irradiating the cell. The scheme for this purpose is shown in Figure (27).

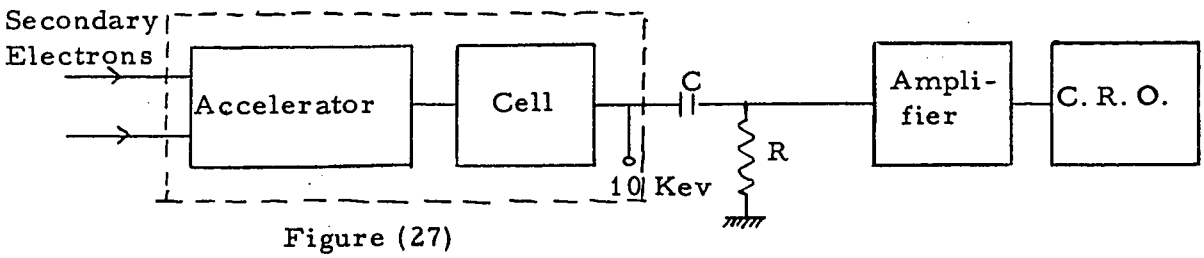

Figure (27)

Since the specimen is at ground potential, both accelerating electrode and the cell have to be at the potential of 10 KeV. And the signal generated will have this voltage as a reference. But, since the scanning frequency is to be above 30 cps, RC coupler as shown in Figure (27) can be used to feed the signal to the amplifier.

5.2 Conclusions:

The research has demonstrated that two types of semiconductor cells, p-n junctions and metal-semiconductor junctions, can be used as detectors of directly reflected electrons in electron scanning microscopes. It has been shown, both theoretically and experimentally, that there is an electron multiplication process when electrons with energies of several KeV produce many electron hole pairs in the semiconductor. Other desirable features of these cells are their small size, convenience and low threshold energy.

The cells have dark currents in the range 10^{-6} - 10^{-7} amperes. For typical back-scattered electron currents in scanning electron microscopes of 10^{-8} - 10^{-9} Amperes and a beam voltage of 20 KeV, an amplification factor 2000 is expected. Thus a contrast ratio of 1: 100 can be obtained.

5.3 Further Work:

This thesis is primarily concerned with the application of semiconductor cells as detectors of directly reflected electrons in scanning electron microscopes and the cells to which the theory and measurements relate are p-n junctions and metal-semiconductor junctions. Brief mention is made of metal-oxide-semiconductor cells, but there is no analysis or measurements. Because of the low dark current, they appear to have some advantages and a complete treatment might be valuable. Also, since there is no full analysis of semiconductor cells as detectors of secondary electrons, (energy less than 50 ev), this might be examined.

The electron multiplication process, in the above cells, might be the basis of several new types of amplifier. An electron flux might be modulated and accelerated, as in a vacuum triode, and a semiconductor cell used as the anode. Then amplification could result from both the modulation by the grid and electron multiplication in the anode.

References:

(1) T. E. Everhart, "Simple theory concerning the reflection of electrons from solids", J. A. P., vol 31, pp. 1483-90, Aug. 1960.

(2) (a) K. C. A. Smith and C. W. Oatley, "The scanning electron microscope and its field of application", Brit. J. A. P., vol. 6, pp 373-376, Nov. 1955.

(b) I. M. Mackintosh, "Applications of the scanning electron microscope to solid state devices", Proc. I. E. E. E., vol , pp 370-377, April 1965.

(c) W. Samaroo, " The Multipurpose Microelectronic Processor", Ph. D thesis, Dept. of Elect. Engg., Univ. of Ottawa, Ottawa, 1965.

(3) O. C. Wells et al, "Factors affecting contrast and resolution in the scanning electron microscope", Journal of Electronics and Control, vol 7, pp 97-111, 1960.

(4) (a) P. Rappaport et al "The electron voltaic effect", RCA Review, vol 17, pp 100-126, March 1956.

(b) D. E. Sawyer et al "Narrow base Germanium Photodiode", Proc. IRE., vol , pp 1123 to 1130, June 1960.

(c) A. G. Jordan et al "Photoeffect on diffused p-n junctions with integral field gradients" IRE Trans. on Electron Devices, vol. ED-7, pp 242-251, October 1960.

(d) L. P. Hunter, Handbook of semiconductor electronics McGraw-Hill Book Co., Inc., Chapter 5, 1962.

(e) M. Woolf, "Drift fields in Photovoltaic solar cells" Proc. IEEE, vol. 51, pp 674-693, May 1963.

(5) P. Rappaport, " Photovoltaic Effect and its utilisation", R. C. A. review, Vol 20, pp. 379-398, Sept. 1959.

(6) R. Williams, "Photoemission of electrons from silicon into silicon dioxide", Phy. Rev., vol 140, 2A, pp 569-575 Oct. 1965.

(7) (a) J. B. Birks, Scintillation Counting, McMillan Co., pp 103-104 and pp 156 to 157, 1964.

(b) T. E. Everhart et al "Wideband detector for micro-microampere low energy electron currents" Journal of Sci. Inst., vol 37, pp 246-248, July 1960.

(8) K. G. McKay, "Electron-hole production in Germanium by Alpha particles", Phy. Rev. vol 84, pp 829-33, November 1951.

(9) K. G. McKay et al, "Electron multiplication in Si and Ge ", vol 91, pp 1079-84, September 1953.

(10) W. Shockley,"Electron-holes in semiconductors," Van Nostrand Company Inc., 1950, p. 315.

(11) W. Prince et al, "New development in silicon photovoltaic devices", Jour. Brit. IRE, pp 583-594, October 1958.

(12) P. Rappaport, "Minority carrier life time in semiconductors as sensitive indicator of radiation damage", Phy. Rev., vol 94, pp 1409-10, June 1954.

(13) P. Rappaport, "The electron voltaic effect in p-n junctions induced by β particle bombardment", Phy. Rev. vol 93, p. 246, January 1954.

(14) W. Ehrenberg et al, "The electron voltaic effect", Proc. Phy. Soc. London, vol 64, page 424, April 1951.

(15) S. Kimoto et al, "The Back-scattered Electron Image of the Electron probe x-ray Microanalyzer using a silicon p-n junction as a detector", Pittsburgh Conference on analytical chemistry and applied spectroscopy; March 6, 1964.

(16) K. Nakamuru et al, "Current amplification of Electron bombardment in the semiconductor barrier layer" J. Phys. Soc. Japan, vol 13, Page 223, 1958.

(17) B. M. Schumacher, "A review of the (Macroscopic) laws for electron penetration through matter" Department of Physics, Ontario Research Foundation pp 28-29, May 1964.

(18) M. Woolf, "Limitations and possibilities for improvement of photovoltaic solar energy converters", Proc. IEEE, vol 48, pp 1240-61, May 1960.

APPENDIX

Criteria for the selection of an electron detector:

The thesis is concerned with the choice of an electron detector for electron scanning microscopes. The output signal of such a microscope may result from either back-scattered high energy electrons or secondary emitted low energy electrons, but the thesis is concerned only with the former. There are several presentations possible from the high energy electrons, two of which are of interest.

(1) The integrated back-scattered electron flux yields information about the atomic number and chemical composition of the specimen.

(2) The differential image yields information about surface topography.

Obtaining the above, requires flexibility in the placing of the electron detectors. Thus it is important that any detector chosen is small and has a large capture area for the space it occupies. In addition, the detector must have adequate sensitivity and stability to produce a useable image on the display.

Comments are made in the thesis regarding the relative advantages of different detectors and their properties. A discussion of these properties and their importance follows.

The desirable properties of electron detectors in scanning electron microscopes are:

1) Convenience, (as discussed above)
2) Sensitivity,
3) Stability,
4) Gain,
5) Frequency response.

Sensitivity:

The sensitivity of a detector is a measure of the minimum useful signal it can detect. It is therefore related to the noise figure and stability, but must not be confused with the gain. The definition of sensitivity used in the thesis is that it is the electron flux required to produce a signal at the output equal to the noise in the system. This noise includes that generated in the detector and any electronics (eg: amplifiers) associated with it. Thus if the detector has a large gain in itself, the requirements of the other electronics are less stringent. There are several forms of noise to be considered dependent upon the way the detector is used.

(1) If the detector is used as a particle counter, only impulsive noise needs to be considered.

(2) If the detector is used to measure the integrated electron flux both dc and ac components of the noise must be considered. Since the dc component, or saturation current, predominates, it alone is measured and the sensitivity is related to this component.

Stability:

If accurate measurements are to be made, stability is desirable. ie. The relation between the output and the electron flux should be predictable . Stability is related to noise, but these two quantities are kept separate in the thesis.

Gain:

Gain is a useful property of a detector, but is of only secondary importance to sensitivity, providing the signal output of the detector is greater than the noise at the input of a low noise amplifier. If the signal is lower than the noise, the sensitivity is directly dependent on the detector gain. However, in all cases detector internal gain reduces the requirements of the electronics in the overall system.

Frequency response:

The frequency response of a detector controls the rate of information flow. Since wide bandwidth amplifiers and display systems are available, the detector response determines the picture detail and repetition time of a scanning microscope. The rate of information flow is also determined by the signal to noise ratio, so that the bandwidth of the detector is important only when the signal to noise ratio is adequate.

VITA

Name: Pappu Venkata Ramana

Born: Chittoor, Andhra Pradesh, India.
May 14th, 1940.

Educated:

Pre-University: Government Arts College
Rajahmundry, India.

University: Birla Institute of Technology
Pilani, India.
Poona University, Poona, India.
University of Ottawa,
Ottawa, Canada.

Course: Electrical Engineering.

Degrees: B.E.
M.Sc. (Poona).